Chromosomal Inversions and Their Potential Impact on the Evolution of Arboviral Vector *Aedes aegypti*

Jiangtao Liang [1,2], Noah H. Rose [3,4,5], Ilya I. Brusentsov [1,2,6], Varvara Lukyanchikova [1,2], Dmitriy A. Karagodin [6], Yifan Feng [1,2], Andrey A. Yurchenko [1,2], Atashi Sharma [1,2,7], Massamba Sylla [8], Joel Lutomiah [9], Athanase Badolo [10], Ogechukwu Aribodor [11], Cassandra Gonzalez Acosta [12], Barry Wilmer Alto [13], Nazni Wasi Ahmad [14], Elina M. Baricheva [6], Zhijian Tu [2,15], Diego Ayala [16,17,18], Andrea Gloria-Soria [19], William C. Black [20], Jeffrey R. Powell [21], Igor V. Sharakhov [1,2,22], Carolyn S. McBride [3,4], Maria V. Sharakhova [1,2,6,*]

[1]Department of Entomology, Virginia Polytechnic Institute and State University, Blacksburg, VA, USA
[2]Fralin Life Science Institute, Virginia Polytechnic Institute and State University, Blacksburg, VA, USA
[3]Department of Ecology and Evolutionary Biology, Princeton University, Princeton, NJ, USA
[4]Princeton Neuroscience Institute, Princeton University, Princeton, NJ, USA
[5]Department of Ecology, Behavior, and Evolution, University of California San Diego, La Jolla, CA, USA
[6]Laboratory of Cell Differentiation Mechanisms, Institute of Cytology and Genetics, Novosibirsk, Russia
[7]Genome Technologies, The Jackson Laboratory, Bar Harbor, ME, USA
[8]Department of Livestock Sciences and Techniques, Sine Saloum University El Hadji Ibrahima NIASS, Kaffrine, Senegal
[9]Arbovirus/Viral Hemorrhagic Fevers Laboratory, Center for Virus Research, Kenya Medical Research Institute (KEMRI), Nairobi, Kenya
[10]Laboratory of Fundamental and Applied Entomology, Université Joseph Ki-Zerbo, Ouagadougou, Burkina Faso
[11]Department of Zoology, Nnamdi Azikiwe University, Awka, Anambra State, Nigeria
[12]Centro Nacional de Programas Preventivos y Control de Enfermedades (CENAPRECE), Vector-Borne Disease Program, Mexico City, Mexico
[13]Entomology and Nematology Department, University of Florida, Institute of Food and Agricultural Sciences, Florida Medical Entomology Laboratory, Vero Beach, FL, USA
[14]Institute for Medical Research, National Institutes of Health, Ministry of Health, Kuala Lumpur, Malaysia
[15]Department of Biochemistry, Virginia Polytechnic Institute and State University, Blacksburg, VA, USA
[16]University of Montpellier, the French National Centre for Scientific Research, the French National Research Institute for Sustainable Development, Montpellier, France
[17]International Center for Medical Research, Franceville, Gabon
[18]Medical Entomology Unit, Institut Pasteur de Madagascar, Antananarivo, Madagascar
[19]Department of Entomology, Connecticut Agricultural Experiment Station, New Haven, CT, USA
[20]College of Veterinary Medicine and Biomedical Sciences, Colorado State University, Fort Collins, CO, USA
[21]Department of Ecology and Evolutionary Biology, Yale University, New Haven, CT, USA
[22]Department of Genetics and Cell Biology, Tomsk State University, Tomsk, Russia

*Corresponding author: E-mail: msharakh@vt.edu.

Accepted: June 02, 2025

Abstract

Chromosomal inversions play a crucial role in evolution and have been found to regulate epidemiologically significant traits in malaria mosquitoes. However, they have not been characterized in *Aedes aegypti*, the primary vector of arboviruses, due to the poor structure of its polytene chromosomes. The Hi-C proximity ligation approach was used to identify chromosomal inversions in 25 strains of *A. aegypti* obtained from its worldwide distribution and in one strain of *Aedes mascarensis*. The study identified 21 multimegabase polymorphic inversions ranging in size from 5 to 55 Mbp. Inversions were more abundant in African than in non-African strains, 15 versus 3 inversions, with the highest number observed in West Africa. All inversions were grouped into two geographic clusters of African or non-African origin, suggesting their association with *A. aegypti* subspecies. Inversions were unevenly distributed along chromosomal arms, with the highest number found in the 1q and 3p arms homologous to the inversion-rich 2R chromosomal arm in the malaria vector *Anopheles gambiae*. Direct comparison of inversions between *A. aegypti* and *An. gambiae* revealed significant overlap in their genomic locations. This finding may explain the parallel evolution of the two species under similar environmental conditions. Some of the inversions colocalized with chemoreceptor genes and quantitative trait loci associated with pathogen infection, suggesting their potential role in host preference and disease transmission. Our study revealed the large pool of structural variations in the *A. aegypti* genome and provides the foundation for future studies of their impact on the biology of this important arboviral vector.

Key words: genome evolution, chromosome rearrangements, disease vector, *Aedes aegypti*, parallel evolution.

Significance

The impact of chromosomal inversions on the evolution of diverse organisms has been demonstrated by previous studies, but they have not been characterized in the arboviral vector *Aedes aegypti* due to the lack of readable polytene chromosomes. Using a genome-based approach, this study identified chromosomal inversions in a wide range of *A. aegypti* strains from around the world and demonstrated that inversions are strongly associated with the geographic origin of the strains and may be involved in subspecies divergence, adaptations to different ecological environments, including adaptations to humans. Our discovery of a large pool of structural variation in the *A. aegypti* genome represents a groundbreaking step forward in our understanding of the genome organization of this important disease vector.

Introduction

Chromosomal inversions are significant contributors to the evolutionary processes in diverse organisms, including plants (Huang and Rieseberg 2020), vertebrate animals (Ferguson-Smith and Trifonov 2007; Kosuthova and Solc 2023; Oliveira da Silva et al. 2024), and insects (Ayala and Coluzzi 2005; Fuller et al. 2019; Jay and Joron 2022). They represent balanced genome rearrangements that involve the reversal of chromosome segments by 180° without significant gain or loss of genetic material. During meiosis, heterozygous crossovers in the inverted region produce inviable gametes with acentric fragments and dicentric chromatids reducing or even eliminating recombination within the inversion, especially around the breakpoints. As a result, an inversion is inherited intact and may lead to the formation of a "supergene" if the region contains multiple divergent alleles of multiple functionally important genes with more pronounced phenotypic effects than those of single genes alone (Thompson and Jiggins 2014; Berdan et al. 2022; Berdan et al. 2023). In the 1930s, T. Dobzhansky conducted pioneering studies on inversion polymorphism in polytene chromosomes in *Drosophila* (Krimbas and Powell 1992). Subsequently, chromosomal inversions have been employed to investigate evolutionary genetics in other Dipteran species with well-developed polytene chromosomes including malaria mosquitoes (Kitzmiller 1976; Stegniy 1991; Coluzzi et al. 2002). Inversions have been demonstrated to influence epidemiologically significant phenotypes in the principal African malaria vector *Anopheles gambiae* (Lanzaro et al. 1998; Coluzzi et al. 2002; Gray et al. 2009; Simard et al. 2009; Ayala et al. 2014; Ayala et al. 2017; Riehle et al. 2017). Nevertheless, the identification of chromosomal inversions in aedine mosquitoes represents a significant challenge due to the large and highly repetitive nature of their genomes (Matthews et al. 2018) and the lack of well-developed polytene chromosomes, which are unsuitable for cytogenetic analyses of the inversions (Campos et al. 2003). Previous genetic mapping experiments have provided indirect evidence of the presence of chromosomal inversions in *A. aegypti* from Senegal (Bernhardt et al. 2009). Two putative chromosomal rearrangements have also been identified in

Senegalese strains of *A. aegypti* using fluorescence *in situ* hybridization (FISH) (Dickson et al. 2016). More recently, linked-read genomic sequencing has indicated the potential presence of multiple microinversions in nine strains of *A. aegypti* (Redmond et al. 2020). However, the extent of inversion polymorphism in natural populations of *A. aegypti* remains largely unexplored and requires further investigation.

The *A. aegypti* mosquito transmits numerous arboviral infections with significant impact on human health (Powell 2016b). This species was initially identified as a vector for yellow fever virus, which caused extensive mortality among human populations in the Americas between the 17th and early 20th centuries (Powell 2016a; Fijman and Yee 2022). Later, the advent of an effective vaccine led to a significant reduction in the prevalence of the disease, but since the 1950s, another disease transmitted by *A. aegypti*, dengue fever, rapidly spread across the globe and became the leading arboviral disease of the 21st century (Gubler 2012). Dengue is now endemic in 100 countries, with an 8-fold increase in incidence over the past two decades, largely due to human activities and associated environmental changes (WHO 2022). Additionally, chikungunya and Zika fevers are two other diseases of growing concern that are transmitted by *A. aegypti* (Nabel and Zerhouni 2016; Powell 2016a). In 2015, an epidemic outbreak of the Zika virus occurred in Brazil, resulting in 1.5 million cases which correlated with over 5,000 instances of uncommon microcephaly in newborns (Faria et al. 2016; Weaver et al. 2016). Because *A. aegypti* is distributed across the global tropics and subtropics and thrives in human environments (Powell 2016a), the diseases associated with this mosquito currently threaten half of the world's human population (Olagnier et al. 2016; WHO 2022). This raises concerns about the risk of new epidemics caused by *A. aegypti* in the future (Fontenille and Powell 2020). Therefore, it is important to gain a deeper understanding of the genetic diversity associated with the ecological plasticity of this species to facilitate the implementation of vector control measures and mitigate arbovirus transmission.

Due to its wide geographic distribution, *A. aegypti* exhibits a high degree of genetic and phenotypic diversity and comprises two subspecies *A. aegypti aegypti* (*Aaa*) and *A. aegypti formosus* (*Aaf*). The subspecies differ dramatically from each other in terms of body coloration, behavior, habitats, association with humans, and ability to transmit pathogens (Mattingly 1957; Sylla et al. 2009; McBride et al. 2014; Powell et al. 2018; Aubry et al. 2020), but no reproductive barriers between the subspecies have been detected in the laboratory experiments (More 1979; McBride et al. 2014). The *Aaf* subspecies is a dark, sylvan form found in sub-Saharan Africa in a variety of environments, including forest, rural, suburban, and urban settings (Powell and Tabachnick 2013; Tabachnick 2013; McBride et al. 2014; Rose et al. 2020). In contrast, the *Aaa* subspecies is a lighter form predominantly found outside of Africa and is strongly associated with human environments. It has been proposed that the human-associated lineage originated in Africa in response to prolonged dry seasons in the Sahel region of West Africa about 5000 years ago when the Sahara expanded and water stored by humans became the main aquatic niche available to mosquitoes (Powell et al. 2018; Rose et al. 2020; Rose et al. 2023). This human-associated "proto-*Aaa*" lineage is believed to have subsequently migrated to the Americas on ships during the trans-Atlantic slave trade in the 1500 s (Brown et al. 2011; Powell and Tabachnick 2013; Brown et al. 2014; Gloria-Soria et al. 2016; Powell et al. 2018). Chromosomal inversions may play a role in the rapid differentiation of the *A. aegypti* subspecies, particularly in adaptation to human hosts and habitats.

The *A. aegypti* subspecies exhibit notable differences in their blood feeding preferences (McBride 2016) and susceptibility to various arboviral infections (Souza-Neto et al. 2019). While *Aaf* has opportunistic host choice and its feeding behavior likely depends on host availability, *Aaa* is strongly anthropophilic. Interestingly, genome comparisons of multiple strains of *A. aegypti* with different origins identified several key chromosomal regions associated with specialization to humans (Rose et al. 2020). Vector competence studies have shown that *Aaa* is a better vector of arboviruses than *Aaf* (Lorenz et al. 1984; Tabachnick et al. 1985; Wallis et al. 1985; Sylla et al. 2009; Aubry et al. 2020), but exceptions have been documented (Sylla et al. 2009; Dickson et al. 2014). Furthermore, an integration of physical and linkage maps indicated the presence of five chromosomal clusters of QTL related to different infections, suggesting that the transmission of different pathogens may be controlled by the same genomic loci (Timoshevskiy et al. 2013). Thus, chromosomal inversions may be associated with epidemiologically relevant phenotypes in *A. aegypti* mosquitoes.

The observed prevalence of inversions in different *Anopheles* species suggests that inversions harboring orthologous genes may also be involved in similar adaptations. Indeed, it has been demonstrated that polymorphic inversions on the 2R arm of *An. gambiae* and on the homologous arms of *Anopheles funestus* and *Anopheles stephensi* nonrandomly shared orthologous genes and also involved in similar environmental adaptations in these three species (Sharakhova et al. 2011b). However, it remains unknown whether such a pattern will be observed between phylogenetically distant species such as *An. gambiae* and *A. aegypti* which share a similar range of geographic distribution that is largely restricted to the tropics. Even though these two species split ~135 million years ago, they have similar chromosome arrangements (Ryazansky et al 2024). The chromosomal complement in both species consists of three pairs of chromosomes in both species, but unlike in

Anopheles, there are no typical heteromorphic X and Y sex chromosomes in *A. aegypti* and sex is determined by a sex locus located on homomorphic chromosome 1, which is morphologically indistinguishable between the sexes (Matthews et al. 2018). In *A. aegypti* all chromosomes are metacentric, with chromosomes 1, 2, and 3 being the smallest, largest, and intermediate, respectively, and with arms approximately equal in length (Sharakhova et al 2011a). The inversion-rich 2R in *An. gambiae* is homologous to the 1q and 3p arms due to a large intrachromosomal translocation (Arensburger et al. 2010; Timoshevskiy et al. 2014).

The availability of a high-quality reference genome for *A. aegypti* (Matthews et al. 2018) now provides an opportunity to employ genome-based technologies for the detection of chromosomal inversions in natural populations of this mosquito. One suitable method is Hi-C proximity ligation. In contrast to microscopy, this approach belongs to the molecular-based 3C (Chromosome, Conformation, Capture)-group of methods (Dekker et al. 2002) and provides insights into the 3D organization of whole genomes (Lieberman-Aiden et al. 2009; van Berkum et al. 2010). The occurrence of specific inter- and intrachromosomal interactions and chromosomal rearrangements, including deletions, inversions, and translocations, can be estimated by measuring the frequency of physical contacts between specific genomic loci within the nuclear space (Engreitz et al. 2012; Chakraborty and Ay 2018; Harewood et al. 2017). The specially developed Hi-C software, Juicebox (Durand et al. 2016; Robinson et al. 2018), provides visualization of different types of interactions on Hi-C heat-map plots. Hi-C maps display short-distance interactions as a distinct diagonal line, while long-distance interactions appear as bright spots that deviate from the diagonal. In the cases of inversions, the areas interacting within the nuclear space are observed away from the diagonal line. This method was successfully used to identify previously known inversions in *Anopheles coluzzii* and *An. stephensi* (Lukyanchikova et al. 2022b) and precise breakpoint positions in the *An. gambiae* genome (Corbett-Detig et al. 2019). Furthermore, this method revealed two previously unknown chromosomal inversions in *Anopheles atroparvus* and *Anopheles merus* (Lukyanchikova et al. 2022b).

In this study, we employed the Hi-C proximity ligation method on pools of individual mosquitoes to identify chromosomal inversions in a panel of *A. aegypti* strains representing a broad range of their global distribution as well as extensively utilized laboratory colonies and a closely related species, *Aedes mascarensis* using the AaegL5 genome assembly (Matthews et al. 2018) as a reference. Our work aims at (i) identifying rearrangements in *A. aegypti* genome; (ii) validating them through FISH; (iii) characterizing their geographic distribution; (iv) testing if inversions overlap with regions of the genome previously shown to be associated with olfaction and vector competence; and (v) analyzing the homology of inversions between *A. aegypti* and *An. gambiae*.

Results

Inversion discovery using Hi-C approach

Here, we used Hi-C technology to discover chromosomal rearrangements in *A. aegypti*. We tested 23 recently colonized strains of *A. aegypti*, of which 11 strains were from five non-African countries and 12 strains were from Africa, two laboratory strains LVP and RU3, and *A. mascarensis* (supplementary table S1, Supplementary Material online, see Methods section for details). According to WGS (Rose et al. 2020), all strains outside of Africa were identified as subspecies Aaa (supplementary table S1, Supplementary Material online). In Africa all strains were Aaf subspecies with variable degrees of Aaa admixture (supplementary table S4, Supplementary Material online, see Methods for details). The exceptions were strains K2 in Kenya and NGO in Senegal, which were identified as subspecies Aaa. These strains had a high degree of Aaa admixture (>37%), morphological scaling patterns characteristic of *Aaa* and showed a preference for humans, like the invasive *Aaa* populations. Inversions and putative misassemblies found in this study are summarized in Table 1. They were recognized based on a butterfly-like pattern outside of the major diagonal in the Hi-C heatmap. The butterfly wing triangles connect at a point that marks the break points, with the color intensity increasing as a gradient from the base to the center of the triangles (Fig. 1, supplementary fig. S1, Supplementary Material online). Figure 1 shows examples of the Hi-C results for chromosomal inversions in chromosome 1 (1pA, 1qD, 1qE, 1qF, 1qG) and misassembly 2. The coordinates of the inversion breakpoints were determined based on the center position of the butterfly-like pattern at a resolution of 5 kb. The lengths of inversions were determined based on breakpoint coordinates (Table 1). For some widespread inversions, such as 1pA, we observed variations in the shape and intensity of the butterfly-like pattern across strains, possibly related to the frequency of the inverted karyotype in the pool of sequenced individuals (Fig. 1a and b). Overall, a higher abundance of individuals with the inversion resulted in a stronger and more intense butterfly-like pattern outside of the diagonal. After evaluating the Hi-C maps of all the strains collected from the field, the old laboratory strains, and *A. mascarensis*, we concluded that, according to our criteria, none of the inversions resulted in a complete disruption of the major diagonal for all the examined strains. Therefore, we classify all the inversions discovered in this study as polymorphic.

Strikingly, a puzzle of four overlapping inversions—1qD, 1qG, 1qE, and 1qF—was found in the telomere region of

Table 1 Chromosomal inversions in *A. aegypti* and *A. mascarensis*

No.	Inversion name	Start (bp)	End (bp)	Length (bp)	Hi-C ID
Field collected strains of *Aedes aegypti*					
1	1pA	1,200,000	16,520,000	15,320,000	MIN; NGO; PKT; OGD; OHI; AWK; FCV; UGA; KAK
2	1pB	71,280,000	104,960,000	33,680,000	F54; T51
3	1qC	208,925,000	223,850,000	14,925,000	OHI
4	1qD	301,350,000	307,420,000	6,070,000	MIN; NGO; PKT; OGD; AWK
5	1qE	265,960,000	308,045,000	42,085,000	MIN; PKT
6	1qF	266,010,000	285,565,000	19,555,000	MIN; PKT; OHI
7	1qG	271,675,000	286,750,000	15,075,000	OGD
8	2pA	59,650,000	103,875,000	44,225,000	B53
9	2qB	298,150,000	332,420,000	34,270,000	OHI
10	2qC	413,890,000	426,620,000	12,730,000	FCV
11	2qD	464,175,000	472,750,000	8,575,000	AWK; KAK
12	3pA	68,700,000	93,800,000	25,100,000	UGA
13	3pB	53,450,000	108,225,000	54,775,000	OGD
14	3pC	80,775,000	97,425,000	16,650,000	MONT, GUER, CUER, COLI
15	3pD	101,800,000	109,600,000	7,800,000	OGD
16	3pE	129,400,000	160,150,000	30,750,000	NGO
17	3qF	328,850,000	337,550,000	8,700,000	UGA
18	3qG	404,100,000	409,300,000	5,200,000	MIN; NGO; PKT; OGD; OHI; AWK; UGA; KAK
Lab strains of *Aedes aegypti*					
1	2qL	377,685,000	379,125,000	1,440,000	LVP
2	3qR	205,905,000	206,750,000	845,000	RU3
Aedes mascarensis					
1	2pM	84,745,000	90,695,000	5,950,000	MASC
#	Misassembly name	Start (bp)	End (bp)	Length (bp)	Hi-C ID
Misassemblies					
1	1p Misassembly 1	193,140,000	194,125,000	985,000	All strains
2	1q Misassembly 2	301,900,000	307,225,000	5,325,000	All strains

Start and end inversion coordinates are shown in accordance with AaegL5.0 genome assembly (Matthews et al. 2018).

the 1q chromosome arm (Fig. 1c and d). Although inversions 1qD, 1qF, and 1qG were found as separate inversions in different strains (Table 1, Fig. 1c), inversion 1qE was always present together with 1qD and 1qF (e.g. in MIN and PKT, Senegal), representing an example of a triple inversion (Fig. 1d). This result suggests that inversion 1qE (42 Mb long) was originally formed on the chromosome that contained both smaller inversions 1qD (5 Mb long) and 1qF (19 Mb long) (Fig. 1c and d). Therefore, inversions 1qE and 1qF formed a "broken butterfly-like" pattern in the Hi-C map of the MIN strain (Fig. 1d) because the proximal breakpoints of the 1qE and 1qF inversions were very close to each other (≈50 kb). Inversion 1qD in the same Hi-C map in the MIN strain formed a clear independent butterfly-shaped pattern because the distal breakpoints of inversions 1qD and 1qF were further from each other (≈625 kb). None of the described inversions shared breakpoints.

Finally, our study identified two misassemblies in the reference genome AaegL5.0 (Matthews et al. 2018). The presence of misassemblies were considered if the butterfly-like patterns outside of the major diagonal in Hi-C maps were determined in all examined strains (Table 1), including the RU3 strain, which was used for the genome assembly (Matthews et al. 2018). The lengths of misassemblies 1 and 2 were 0.98 Mb and 5.3 Mb, respectively. The larger misassembly 2 was located near inversion 1qD but had slightly different coordinates and was clearly differentiable in both the OGD and MIN strains in Fig. 1c and d, respectively.

Overall, based on Hi-C data, our study discovered 18 chromosomal inversions in recently colonized strains from around the world, 2 inversions in old laboratory strains, Liverpool (Severson et al. 2002) and the inbred derivative strain RU3 (Matthews et al. 2018), 1 inversion in *A. mascarensis*, and 2 potential misassemblies in the reference genome AaegL5.0 (Matthews et al. 2018).

Inversion validation using fluorescence *in situ* hybridization

To validate the Hi-C results, chromosomal inversions were examined using FISH in mitotic chromosomes from imaginal discs of 4th instar larvae. Six inversions (1pA, 1qD, 1qE, 1qF, 3pA, 3pB) and misassembly 2 were selected for validation based on their abundance, geographical distribution,

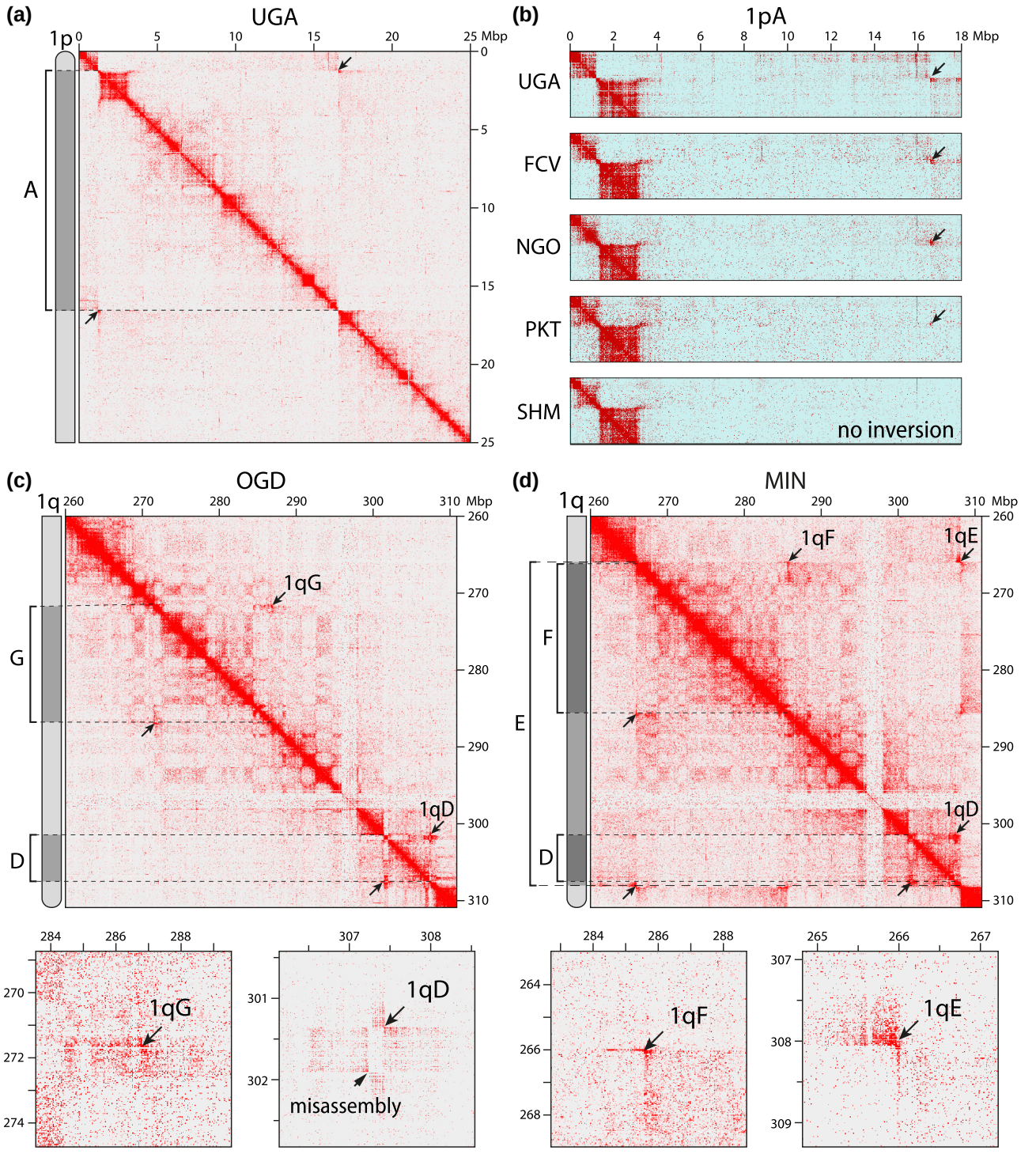

Fig. 1. Inversion patterns in the Hi-C heat maps of the chromosome 1. a) Hi-C heat map for the 1pA inversion in the UGA strain. b) Different patterns of Hi-C heat maps associated with frequencies of the 1pA inversion in different strains. c) Hi-C heat map for the 1qG and 1qD inversions and misassembly 2 in the OGD strain. d) Hi-C heat map for three overlapping inversions, 1qD, 1qE, and 1qF inversions, in the MIN strain. Schematic representations of inversions are indicated by brackets within the chromosome arms on the left of (a, c, and d). Arrows point to the center of the butterfly-like patterns. Break points are shown by dashed lines. Below the pictures on (c) and (d) are enlarged images of the inversions and misassembly 2. Chromosomal inversions are seen as a butterfly-like pattern outside of the major diagonal on the Hi-C heat maps. These patterns are more pronounced in strains with a higher abundance of individuals carrying inversion 1pA (b). Overlapping inversions 1qE and 1qF produce a disrupted butterfly pattern on the Hi-C heat map shown in (d).

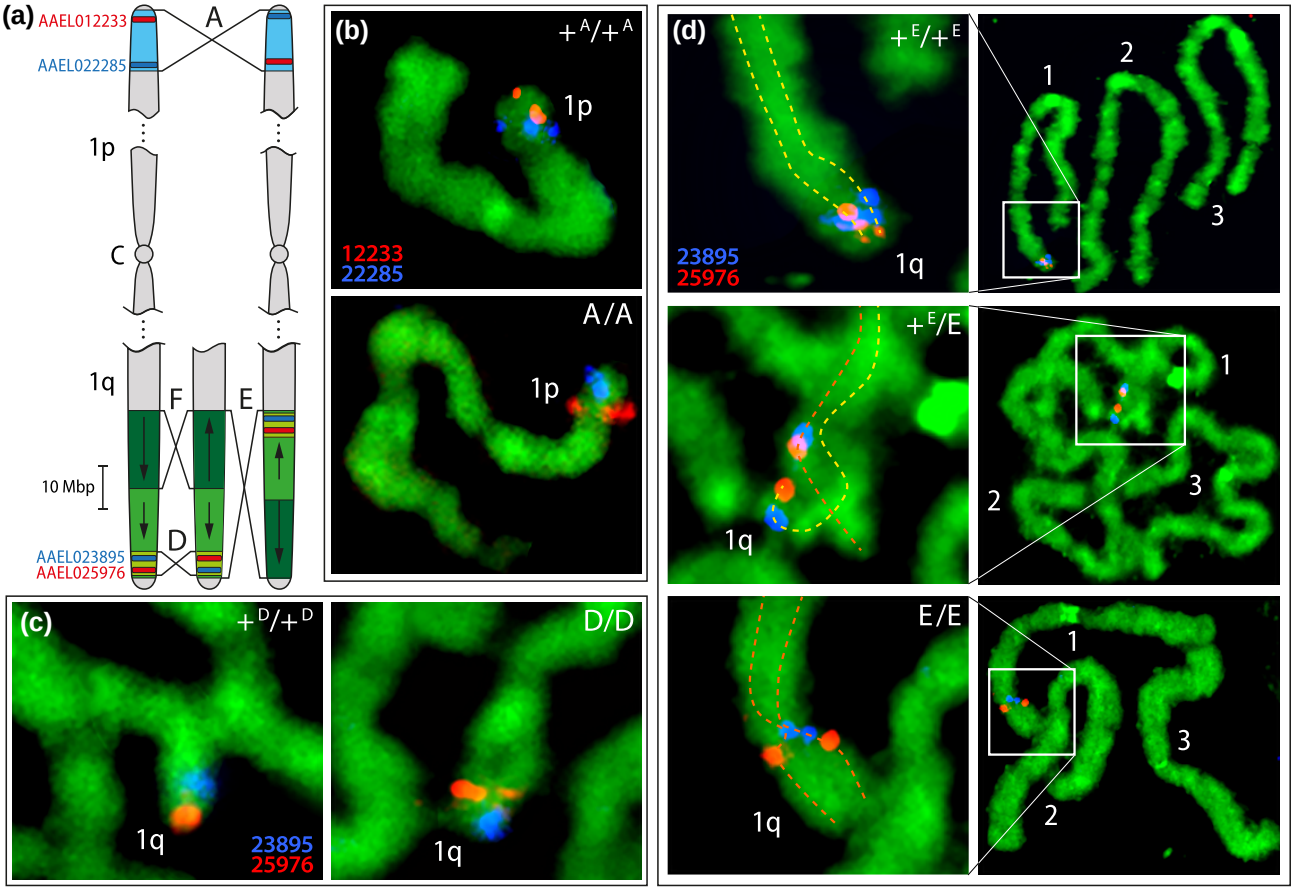

Fig. 2. Validation of inversions in chromosome 1 using FISH. a) A diagram of FISH experiments for chromosome 1. Chromosomes are schematically shown by gray color. Letter C stands for the centromere. Inversion 1pA is shown in blue color, inversions 1qE, 1qD, and 1qF are shown by different shades of green color. Chromosome arms 1p and 1q on the left of the panel represent standard arrangements; chromosome arms in the middle and on the right are shown in inverted arrangements. Arrows inside the inversion regions of 1qE and 1qF indicate orientations of standard arrangements. Positions of probes used for FISH, AAEL012233, AAEL025976 and AAEL022285, AAEL023895, are indicated by red and blue colors, respectively. The corrected pattern of misassembly 2 is shown in supplementary fig. S2, Supplementary Material online. Breakpoint positions are indicated by brackets. b–d) Examples of FISH for validation of the inversions 1pA (b), 1qD (c), and 1qE (d). 1p and 1q stand for the chromosome arms. Numbers 1, 2, and 3 stand for the chromosome numbers. All images represent chromosomes at the prometaphase stage of mitosis whereas homologous chromosomes are paired. Standard arrangements of the chromosomes are indicated as +, inverted by capital letters A, D, and E. Probes used for FISH are indicated by the last five numbers in red and blue colors in correspondence with the fluorescence dyes Cy3 (red) or cy5 (blue), which were used for the labeling. Chromosomes are counterstained with YOYO-1 (green). Standard and inverted arrangements are shown for the inversions 1pA (b) and 1qD (c) but standard, inverted, and heterozygous arrangements are shown for the inversion 1qE. In d), images on the left represent zoomed pictures of the images on the right. Homologous chromosomes are tracked by dashed lines in yellow and red for the standard and inverted arrangements in (D). The mosquito strains used in this figure are RU3 for $+^{A}/+^{A}$, UGA for A/A, RU3 for $+^{D}/+^{D}$, OGD for D/D, and MIN for $+^{E}/+^{E}$, $+^{E}$/E, and E/E. FISH results provide physical evidence for the presence of the inversions.

and chromosomal location. Since some of these inversions, as well as misassembly 2, overlapped, we were able to perform FISH using only three pairs of probes: AAEL012233 and AAEL022285 probes for the 1pA inversion, AAEL025976 and AAEL023895 probes for the 1qD and 1qE inversions and the misassembly 2 on the 1q arm, and AAEL007127 and AAEL019648 probes for the 3pA and 3pB inversions (supplementary table S2, Supplementary Material online).

A scheme and examples of FISH experiments in chromosome 1 are shown in Fig. 2. As each of the paired probes was labeled by a different fluorescent dye (Cy3 or Cy5), standard, inverted, and heterozygote karyotypes were identified by the order of the probe signals along the chromosomes based on their proximity to the telomere. For the 1pA inversion, we performed FISH for the RU3, PKT, and UGA strains. FISH results demonstrated that only individuals with standard arrangements were present in the RU3 and PKT strains, but only inverted arrangements were found in all individuals of the UGA strain (Fig. 2, supplementary table S3, Supplementary Material online).

In addition, we examined the presence of misassembly 2 and inversions D and E in the 1q arm. To validate the presence of misassembly 2, we performed FISH of the AAEL023895 and AAEL025976 probes in five individuals from the reference genome strain RU3 (Matthews et al. 2018). In all individuals, FISH results showed the reverse order in the chromosomes compared to the reference AaegL5.0 genome, supporting the presence of a misassembly (supplementary fig. S2, Supplementary Material online). Then, we used the same probes to test for overlap between misassembly 2 and inversion 1qD in 2 different strains, UGA and OGD. The Hi-C data mapped to the reference genome indicated the absence of the 1qD inversion in the UGA strain but the presence of this inversion in the OGD strain and the presence of misassembly 2 in the reference genome (Table 1, Fig. 1c). The FISH results confirmed the absence of the 1qD inversion in the UGA strain and presence of the misassembly in the reference genome. In contrast, FISH results in the OGD strain indicated the presence of only inverted 1qD arrangements in all three tested individuals but also supported the presence of misassembly 2 in the reference genome (Fig. 2c, supplementary table S3, Supplementary Material online).

Finally, we used the same pair of FISH probes, AAEL023895 and AAEL025976, to confirm the presence of 1qE in the PKT and MIN strains. Because inversion 1qE is bigger than inversion 1qD (42 Mb vs. 6 Mb), we were able to use proximity to the telomere as an additional marker for interpretation of the FISH results (Fig. 2a). Standard ($+^{E}/+^{E}$) and inverted (E/E) arrangements were recognized by signal locations near or distant from the 1q telomere, respectively (top and bottom panels, Fig. 2d). The heterozygous arrangement ($+^{E}$/E) is shown in the middle panel of Fig. 2d. In this case, signals were observed in different positions on two homologous chromosomes that were paired at the prometaphase stage of mitosis. FISH results in both the PKT and MIN strains showed the presence of standard, heterozygote, and inverted karyotypes of this inversion (supplementary table S3, Supplementary Material online).

Inversions 3pA in the UGA strain and 3pB in the OGD strain were only found in standard and standard/heterozygous arrangements among four and ten tested individuals, respectively (supplementary table S3, Supplementary Material online, supplementary fig. S3, Supplementary Material online). Thus, FISH results provided clear evidence that the inversions identified by the Hi-C method are real.

Inversion nomenclature and metrics

Because there was no overlap between the inversions we document here and those putatively identified in previous work (Dickson et al. 2016; Redmond et al. 2020), we established a new nomenclature for the discovered inversions. First, the name of each inversion included the name of the chromosomal arm on which it was found, following the nomenclature for *A. aegypti* chromosomes (Sharakhova et al. 2011a). The chromosomal complement in *A. aegypti* consists of three pairs of metacentric chromosomes 1, 2, and 3 with shorter arms p and longer arms q (Fig. 3). In addition to the chromosomal arm, the name of each inversion includes a capital letter (A, B, C, D, etc.) to avoid confusion with previously described putative microinversions that were named by small letters (Redmond et al. 2020).

The chromosomal inversions identified in the field strains were unevenly distributed among chromosomal arms with most of the inversions were found on arms 1q ($n = 5$) and 3p ($n = 5$). Within chromosomal arms, inversions were most dense in the area close to the telomere on arm 1q and in the middle of arm 3p. The lengths of inversions found in recently colonized strains varied from 5,200,000 bp (3qG) to 54,775,000 bp (3pB) with a mean inversion length of 21,971,389 bp and a median inversion length of 15,985,000 bp (Table 1). The length of two inversions found in the old lab strains were smaller—1,440,000 bp for 2qL in the Liverpool strain and 845,000 bp for 3qR in the RU3 strain, respectively. The inversion found on arm 2p (2pM) in *A. mascarensis* has a length of 5,950,000 bp. Thus, our study identified the presence of a large pool of multi-megabase chromosomal inversions in the *A. aegypti* genome with uneven distribution along the chromosomes.

Geographical distribution and population patterns

To better understand the geographical distribution of the chromosomal inversions found in *A. aegypti,* we included multiple strains from across the global tropics in this study. Among 23 recently colonized field strains, 12 strains were from 6 countries in Africa: Burkina Faso, Gabon, Kenya, Nigeria, and Uganda, and 11 strains were from 6 countries outside of Africa: Brazil, Colombia, Malaysia, Mexico, Thailand, and the United States. Overall, the study identified more inversions in African strains than in non-African strains: 15 versus 3 inversions, respectively (Fig. 4). It is encouraging to note that these inversions occur in regions that showed elevated differentiation between populations in previous genomic work (Rose et al. 2020). Among all the inversions found in Africa, three inversions, 1pA and 3qG, were abundant in multiple strains distributed across the continent and, therefore, were classified as common African inversions. Four inversions, 1qD, 1qG, 1qE, and 1qF, were discovered only in West Africa and were classified as West African endemic inversions. Another nine inversions were considered rare because they were found only in one or two African strains. Among three chromosomal inversions in *A. aegypti* outside of Africa, the 3pC inversion was found in four Mexican populations. Intriguingly, inversion 1pB was found in two geographically distant populations in Thailand and in the United States (in Florida),

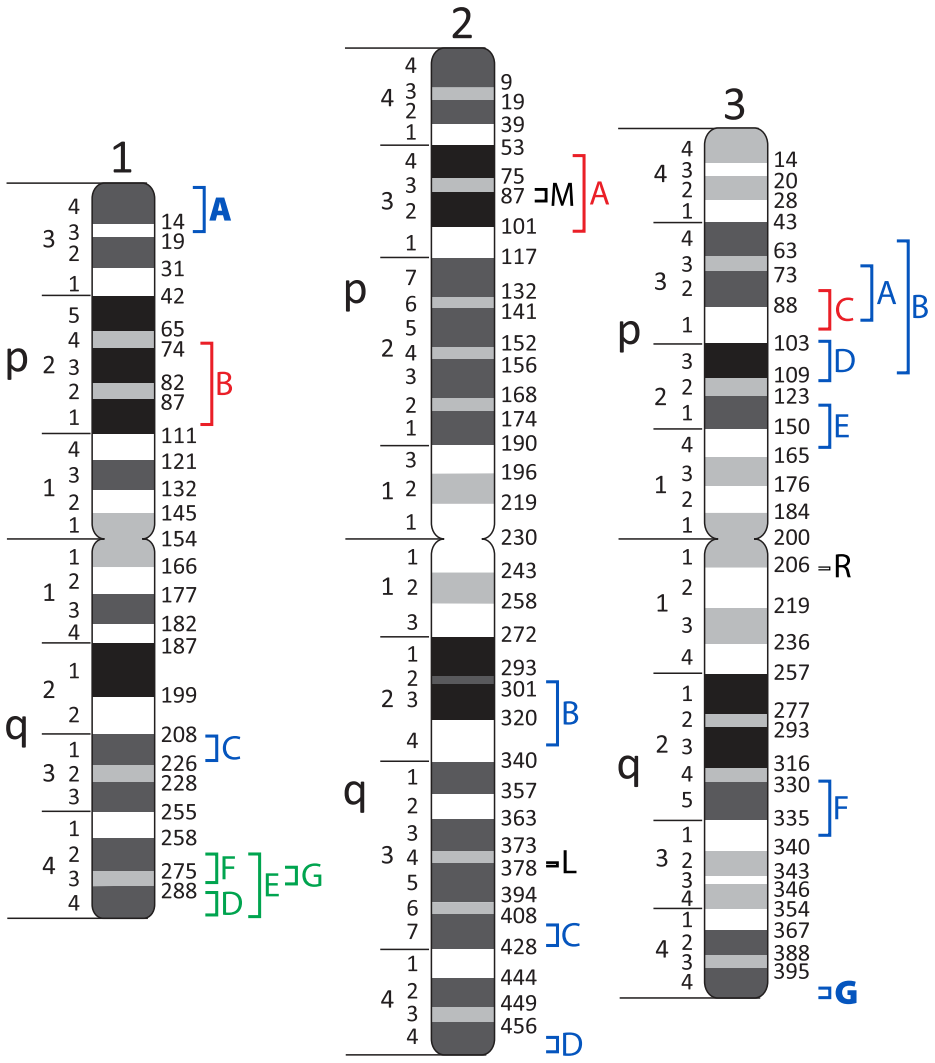

Fig. 3. Chromosomal map of the inversion identified in *A. aegypti* and *A. mascarensis*. Chromosomes are labeled as 1, 2, 3; short and long arms are indicated as p and q, respectively. Numbers on the left indicate chromosome regions and on the right show genome coordinates in Mb in accordance with AaegL5.0 genome assembly (Matthews et al. 2018). Inversions endemic in West Africa, other inversions in Africa, and inversions found outside of Africa are shown by green, blue, and red colors, respectively. Common African inversions 1pA and 3qG are shown in bold. Inversions 2pM in *A. mascarensis*, 3qR and 2qL in RU3 and Liverpool strains are shown black. Inversions are unevenly distributed along the chromosomes whereas most of the inversions localize in the 1q and 3p arms.

suggesting a potential common ancestry of these strains. Only one strain from Africa (SHM in Kenya) and four from outside Africa (two from Florida, United States, one from Colombia, and one from Malaysia) showed no evidence of inversions. Thus, inversions in *A. aegypti* are abundant and highly associated with the geographical location of the strain.

In addition to characterizing the geographical distribution of each inversion based on Hi-C data from lab colonies, we identified the spread of the common inversions, 1pA and 3qG in Africa using SNP-based inversion genotyping approach. For the SNP identification, we used publicly available whole-genome sequences from 393 field-collected individuals from ~30 populations across the African continent (Rose et al. 2020) shown in supplementary table S4, Supplementary Material online. First, to control for the effects of population structure, we examined genetic structure across the two inversion loci within a single geographic region, southern Senegal, which was expected to harbor both inversions at intermediate frequencies. As expected, principal component analyses of inversion loci yielded bi- or trimodal distributions of individuals across the first principal component, likely corresponding to the different inversion karyotypes

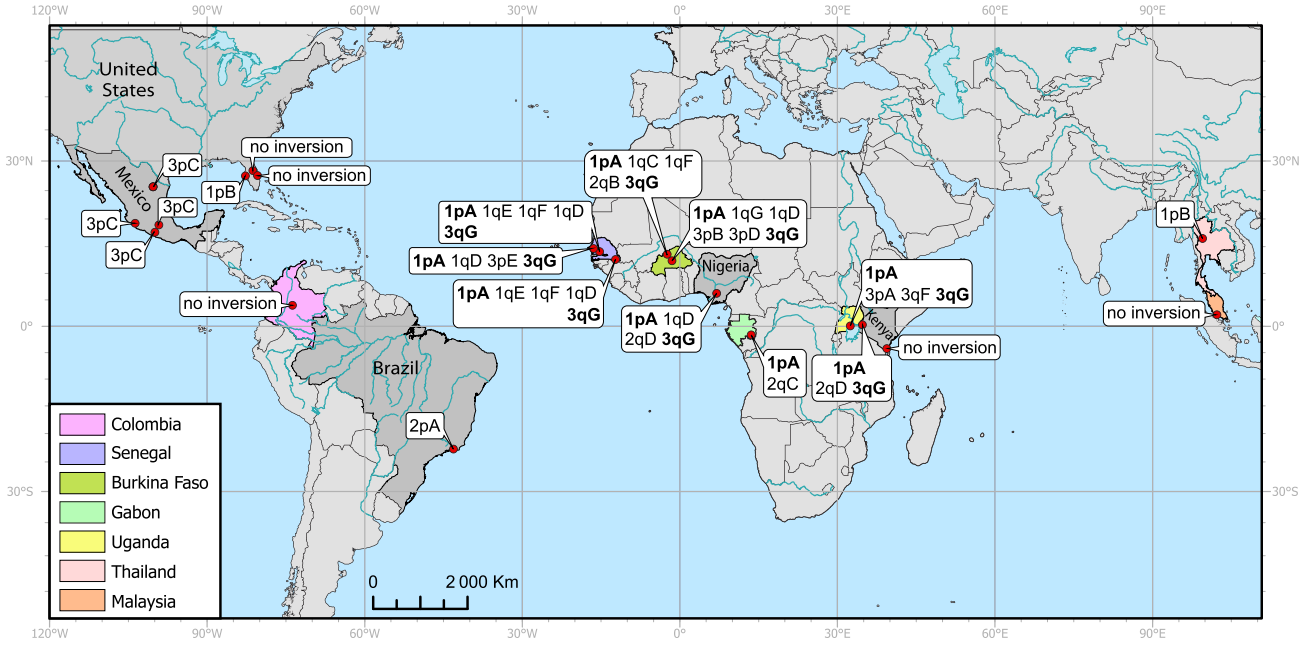

Fig. 4. Geographical distribution of the chromosomal inversions discovered by Hi-C analysis. Common inversions 1pA and 3qG in Africa are shown in bold. Countries are shown by different colors. Inversions are more abundant within Africa than outside of Africa. There is no overlap between African and non-African inversions. Inversions were not present in five locations.

Table 2 Diagnostic SNPs for inversions 1pA and 3qG

Inversion	Inversion genome coordinates (Mb)	Genome coordinates for diagnostic SNPs (bp)
1pA	1.2 to 16.5	16421358, 16422475, 16422651, 16442937, 16443906, 16452597, 16452822, 16452923, 16453689
3qG	404.1 to 409.3	**404145030, 404187138, 404258781, 404266298, 404490025, 404650498**

Genome coordinates are shown according to AaegL5 genome assembly of *A. aegypti* (Matthews et al. 2018). SNPs showing perfect correlation with putative karyotype are shown in bold.

(supplementary fig. S4, Supplementary Material online). The SNPs driving this structure showed strong linkage disequilibrium for multiple places across each inversion locus (supplementary fig. S5, Supplementary Material online), and the consensus genotype across these SNPs for all 393 examined individuals corresponded precisely to the distribution and abundance of inversions found in our Hi-C analyses (Table 1). Finally, we identified putatively diagnostic SNPs with near-perfect correlation to the estimated inversion karyotype (Table 2).

Based on these inversion-linked SNPs, we estimated the frequencies of the standard, inverted, and heterozygote karyotypes for inversions 1pA and 3qG in all 31 populations across Africa. In four African locations, KIN′, OGD′, RAB′, and BUN′, two or three closely located populations with low number of individuals were combined and named by the population with the biggest number of individuals (supplementary table S4, Supplementary Material online, see Method section for details). The results of this analysis are shown in Fig. 5a. We used the chromosomal inversion frequencies of 24 African-wide populations and 2 populations outside of Africa to perform a hierarchical clustering analysis (Fig. 5b. supplementary fig. S6, Supplementary Material online). The analysis subdivided all mosquito populations into four large clusters: (i) Eastern Kenya and non-African locations; (ii) Coastal West Africa; (iii) West-Africa; and (iv) Central Africa. In Africa, most of the populations followed the patterns of their geographical origin with only minor exceptions. The first cluster included five populations from Coastal Kenya (KWA, SHM, RAB′, ABK, GND, and KBO) and two non-African populations from Brazil (SAN), and Thailand (BKK). This cluster was associated with extremely low frequencies or the absence of inversion 1pA and complete absence of inversion 3qG. Exceptionally, a population of Central African origin in Gabon (LPV), which also falls into this cluster, had a low frequency of 1pA inversion and no 3qG inversion. The second cluster included four populations located in coastal areas of West and Central Africa in Senegal (THI and NGO), Ghana (KUM), and Gabon (LBV). In contrast to East Coastal African

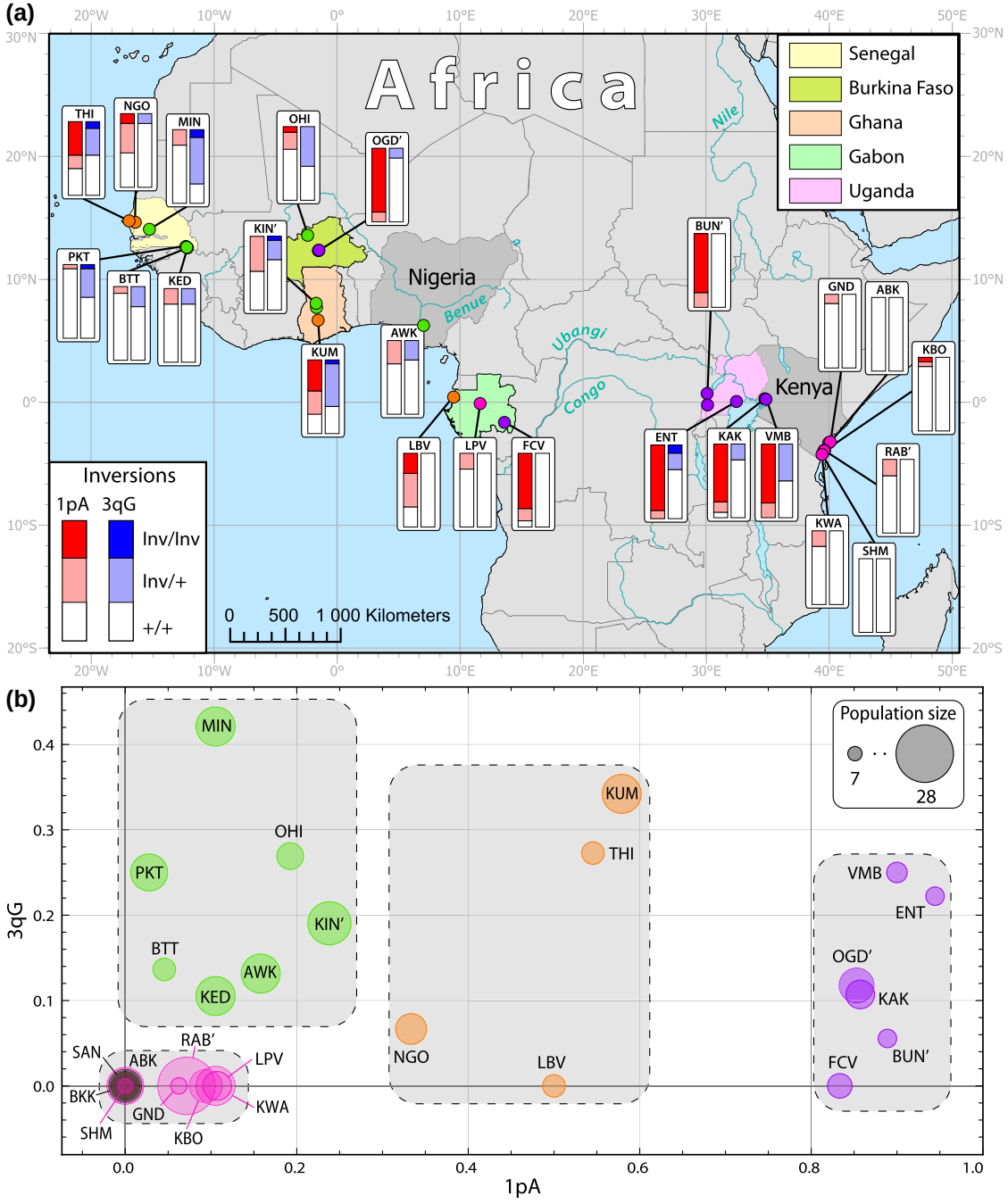

Fig. 5. Frequencies of the chromosomal inversions 1pA and 3qG discovered by SNP analysis in whole-genome sequences of African mosquitoes. a) Frequencies of the inversions in populations across the Africa. Proportions of standard, inverted, and heterozygote arrangements are shown by charts with different colors. Geographical locations are indicated by population ID (supplementary table S4, Supplementary Material online). Countries are shown by different colors. Dot colors indicate correspondence of these locations to four different clusters shown in (b). b) Clusters associated with inversion frequencies. Populations are shown by circles with different colors and are indicated by population ID (supplementary table S4, Supplementary Material online). Population sizes are proportional to the diameter of the circles. Colors of these circles indicate correspondence of this location to the four clusters (supplementary fig. S5, Supplementary Material online) shown by gray rectangles. In four locations, KIN', OGD', RAB', and BUN', 2 or 3 closely located populations with low number of individuals were combined and named by the population with the biggest number of individuals (supplementary table S4, Supplementary Material online). The composition of clusters correlates with the geographic locations of populations. These clusters correspond to the following geographic regions: (1) coastal East Africa (pink) and non-Africa (gray): (2) coastal West Africa (orange); (3) West Africa (green); (4) Central Africa (purple). Mosquitoes from two locations only, OGD (Burkina Faso) and LPV (Gabon), fall into different clusters than expected in accordance with geographical locations: Central Africa and Coastal East Africa/non-Africa, respectively.

populations, 1pA inversion frequencies were relatively high and inversion 3qG was also present. The third cluster included seven populations located in inland West Africa: Senegal (MIN, PKT, BTT, and KED); Burkina Faso (OHI); Ghana (KIN′); and Nigeria (AWK). The presence of both 1pA and 3qG was a characteristic of this cluster. Finally, the fourth cluster included three tropical Central African populations from Uganda (BUN′, KCH, ENT), two from Western Kenya (KAK, VMB), and one from Gabon (FCV). A typical feature of this cluster was extremely high frequencies of the 1pA inversion and the presence of the 3qG inversion. One population from Burkina Faso (OGD′) also fell into this cluster because of the abundance of the 1pA inversion in this population. Thus, chromosomal inversions found in this study are highly associated with the geographic origin of the strains and can be potentially involved in adaptations of *A. aegypti* populations to the natural environment.

Potential associations of the inversions with epidemiologically important traits

To explore the potential contribution of chromosomal inversions into epidemiologically important phenotypes in *A. aegypti*, such as olfactory behaviors or vector competence, we attempted to find colocalizations of chromosomal inversions, chemoreceptor genes, and QTL related to vector competence. Chemoreceptors involved in host seeking behavior of mosquitoes are subdivided into three families: odorant receptors (ORs), gustatory receptors (GRs), and ionotropic receptors (IRs) (Matthews et al. 2018). We calculated an overlap significance between each inversion and the positions of each class of chemoreceptor genes separately (i.e. increasing density of the corresponding genes inside inversions). Using this approach, we identified seven inversions that colocalized with chromosomal positions of chemoreceptor genes with sufficient statistical significance (Fig. 6a, supplementary table S5, Supplementary Material online). West-African overlapping inversions 1qF and 1qE, and Brazilian inversion 2pA colocalized with the OR genes. Mexican inversion 3pC, and overlapping African inversions 3pA, 3pB, and 3pD colocalized with IR genes. Finally, overlapping African inversion 3pB and 3pD also colocalized with the positions of GR genes. We applied the same calculation to find an overlap between inversions and QTL for various infections (Timoshevskiy et al. 2013). The Brazilian inversion 2pA and African inversion 3pB significantly overlapped with QTL related to the transmission by mosquitoes of various infectious disease agents.

Because chemoreceptors are distributed nonrandomly throughout the genome and clustered into chemoreceptor-rich regions, we performed additional calculations to find an overlap between inversions and clusters of evolutionary related chemoreceptors (Ryazansky et al. 2024). We first identified chemoreceptor genes with similar evolutionary trajectories and combined them into evolutionary clusters based on their position on phylogenetic trees and their chromosome positions (supplementary figs. S7 to S9, Supplementary Material online). For example, 60 out of a total number of 106 OR genes were combined into 24 OR gene clusters and 46 remaining genes (supplementary fig. S7, Supplementary Material online, supplementary table S6, Supplementary Material online). When overlaps between inversions and chemoreceptor gene clusters/remining genes were calculated, four inversions were still identified as enriched with these genes: 1qF with OR genes, 1qC with IR genes, and inversions 3pB and 3pD were enriched with GR genes (supplementary table S7, Supplementary Material online). Finally, we employed a permutation test (Cabrera et al. 2012) to validate whether inversion regions were enriched for chemoreceptor genes. We applied 100 circular chromosome permutations, in which a single random offset was drawn from a uniform distribution across the length of each chromosome. Circular permutations also revealed a significant overlap ($P < 0.01$) between inversions and chemoreceptor genes, considering the clustering of chemoreceptor genes within the genome (supplementary fig. S10, Supplementary Material online). Thus, this study demonstrated significant overlap between the genomic locations of the chromosomal inversions and chemoreceptor genes and QTL associated with various infections.

Genetic similarities between inversions in *Aedes aegypti* and *An. gambiae*

It has been shown that the 1q and 3p chromosomal arms in *A. aegypti* are homologous to the inversion-rich 2R arm in the malaria vector *An. gambiae* (Arensburger et al. 2010; Timoshevskiy et al. 2014). In this study, we compared the location of genes inside of the common inversions of *An. gambiae* (Sharakhov et al. 2006; Coulibaly et al. 2007; George et al. 2010; Lobo et al. 2010) (supplementary table S8, Supplementary Material online) with locations of the inversions described in this study for *A. aegypti*. A total of 7,347 single-copy orthologs were identified between the two species and used to test whether inversions in one species significantly overlap with inversions in the other species (Fig. 6b, supplementary fig. S11, Supplementary Material online). The results of the hypergeometric test identified 33 significant associations after multiple testing correction out of total of 126 comparisons. The most significant associations were found between the 3pA (UGA) and 3pB (OGD) inversions of *A. aegypti* and the 2Rj inversions of *An. gambiae*. Also, the 2pA (B53) inversion of *A. aegypti* significantly overlapped with the 2La inversion of *An. gambiae*. Moreover, inversion 3pD in *A. aegypti* significantly overlapped with multiple inversions of 2R chromosomal regions in *An. gambiae* (2Rbk, 2Rc, 2Rd, 2Ru). These results

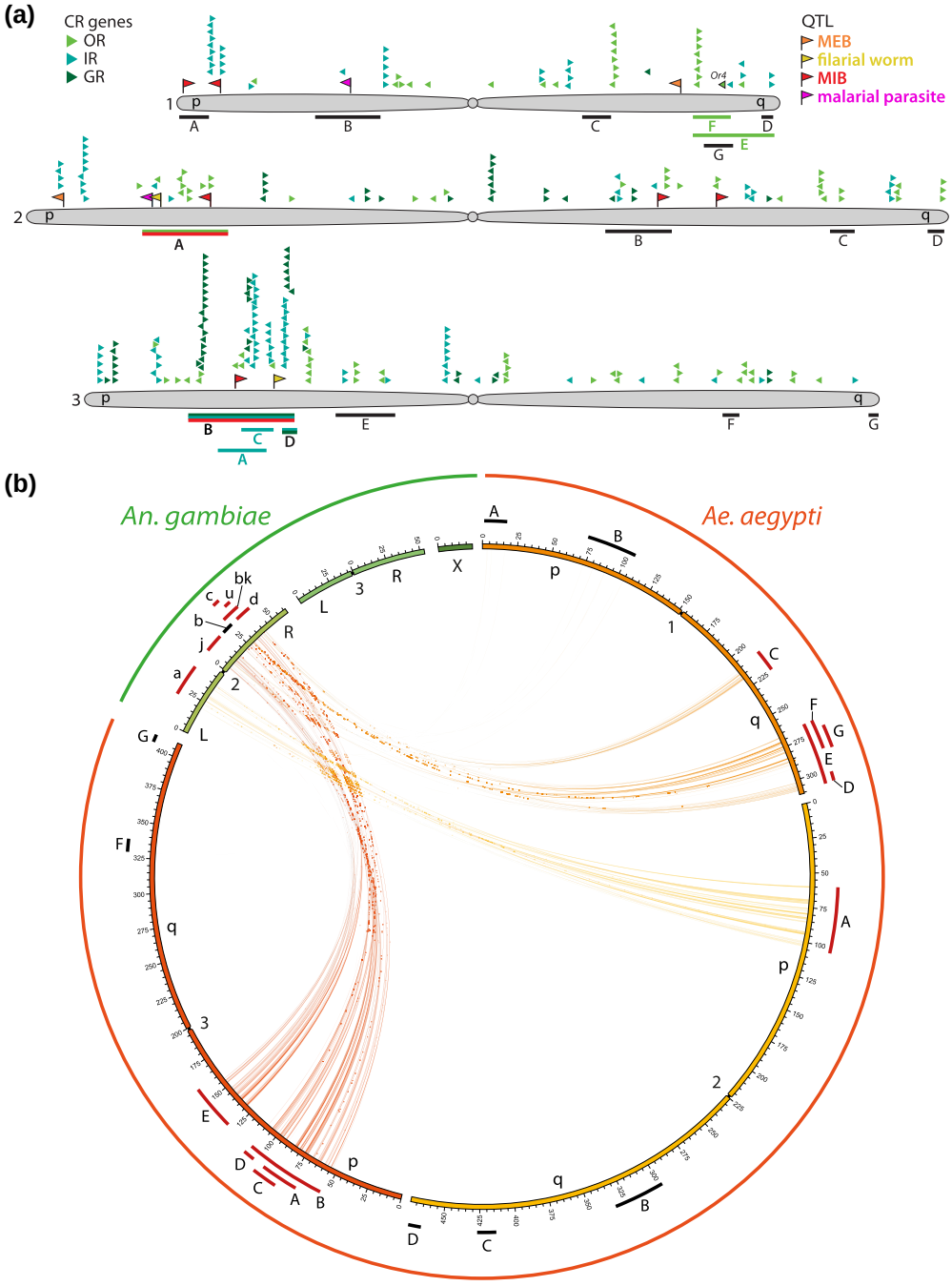

Fig. 6. Associations of the chromosomal inversions *A. aegypti* with chemosensory receptor genes and quantitative trait loci related to vectorial capacity (a) and overlaps with *A. gambiae* inversions (b). a) Chromosomes are indicated by the numbers 1, 2, and 3 and arms as short p and long q. Chromosomal positions and orientation of chemosensory receptor (CR) genes including odorant receptor (OR), gustatory receptor (GR), and ionotropic receptor (IR) genes are shown by small triangles in different colors, with coding strand indicated by the direction that the triangles point. Quantitative trait loci (QTL) are shown by flags in different colors. MIB (midgut infection barrier) and MEB (midgut escape barrier) indicate two different types of QTL related to dengue virus infection. Chromosomal inversions are shown by colored and black lines below the chromosomes. Inversions associated with CR genes and QTL are labeled with the same colors. Seven and two chromosomal inversions overlap with statistical significance with CRs and QTL, respectively. b) Circos plot representation of single copy orthologs between the two species falling into the common regions of inversion polymorphism. Chromosomes are shown by green color for *An. gambiae* and red, orange, and yellow colors for chromosomes 1, 2 and 3 in *A. aegypti,* respectively. Chromosomal inversions with significant overlaps between the species are shown by red bars and the rest of the inversions are indicated by black bars. Lines connect positions of the ortholog genes in the genomes of the two species. Inversion-rich regions in the 1p and 3q arms in *A. aegypti* significantly overlap with inversions in the 2R arm. Widely spread in Africa, inversion 2La of *An. gambiae* overlaps with inversion 2pA found in *A. aegypti* from Brazil. Locations of CR genes and QTL are shown in accordance with AaegL5.0 genome assembly (Matthews et al. 2018).

indicate that common sets of genes between these highly diverged species are nonrandomly implicated in the inversion polymorphism and can potentially be important for their adaptation, suggesting a parallel evolution of the two species under similar environmental conditions (discussed below).

Discussion

Although inversion polymorphism in natural populations is well-characterized in malaria-transmitting *Anopheles* mosquitoes, including the major vector of malaria in Africa, *An. gambiae* (Coluzzi et al. 2002; Love et al. 2016; Love et al. 2020), finding chromosomal inversions in *A. aegypti* has been challenging due to the difficulty of obtaining high quality polytene chromosome preparations from this species (Campos et al. 2003). In this study, for the first time, we document presence of the large chromosomal inversions in the *A. aegypti* genome using a molecular method called Hi-C proximity ligation (Corbett-Detig et al. 2019). The seven inversions identified in our study exhibited positional similarity to those recently discovered in 1206 global WGS on chromosomes 1 and 2, but not on chromosome 3 (Crawford et al. 2024). The WGS analyses revealed the presence of additional inversions that were not identified by the Hi-C method. Indeed, the Hi-C approach is not suitable for identification of microinversions as their butterfly-like pattern, if present, would be located very close to or "buried" inside the main diagonal on the contact heat map if inversion size is under 500 kb. Interestingly, the development of a linkage map based on hybrids between the *A. aegypti* Liverpool strain and the PK-10 strain of *A. aegypti* from Senegal indicated severely reduced recombination in F2 offspring, suggesting the presence of four, one, and three inversions in chromosomes 1, 2, and 3, respectively (Bernhardt et al. 2009). Although the genomic positions of the genetic markers used in the linkage mapping study did not match the inversion positions found here, it is likely that the inversions contribute to reduced recombination in the chromosomes in hybrids between the Liverpool and PK-10 strains.

Since the inversion polymorphism has been well characterized in the African malaria vector, *An. gambiae*, it was interesting to compare the inversions between these two species. The lengths of chromosomal inversions in natural populations of *A. aegypti* varied between 5 and 55 Mb, nearly twice the length of those in *An. gambiae* (4–22 Mb) (Love et al. 2019). Such differences are likely related to the fact that the *A. aegypti* genome is 4.4 times the size of *An. gambiae*, 1.25 Gb (Matthews et al. 2018) versus 0.25 Gb (Holt et al. 2002), respectively. As in the *An. gambiae* genome, inversions in *A. aegypti* were unevenly distributed along chromosomal arms. In *A. aegypti* the highest numbers of inversions were identified in the 1q and 3p arms. In *An. gambiae*, most chromosomal inversions have been found in the arm 2R, which is homologous to both the 1q and 3p arms of *A. aegypti* (Timoshevskiy et al. 2014). Among 15 inversions found in Africa, only two (1pA and 3qG) were common across the entire continent. Likewise, only two *An. gambiae* inversions, 2La and 2Rb, are widely spread in Africa (Love et al. 2019). Most of the endemic chromosomal inversions in *A. aegypti* (1qF, 1qD, 1qE, and 1qG) were found in West Africa. Similarly, three chromosomal inversions (2Rc, d, and u) on the 2R arm of *An. gambiae*, homologous to 1q arm of *A. aegypti*, are restricted to West Africa and only rarely found in Central and Eastern Africa. However, these species comparisons are tentative as much better information on geographical distribution of inversions in *A. aegypti* is needed to reach any strong conclusions.

Nevertheless, it is tempting to speculate that the similar geographic ranges of inversion polymorphisms in two distantly related African mosquito species, *A. aegypti* and *An. gambiae*, are associated with their shared natural environment. If the same genes are captured by inversions in both species, they may have the same phenotypic effects. This study directly examined the overlap between the genes located within *A. aegypti* and *An. gambiae* inversions. Interestingly, multiple genes inside of the endemic West African *An. gambiae* inversions 2Rc, 2Rd, 2Ru (Love et al. 2019) overlapped significantly with the 3pD inversion of *A. aegypti*, which is also endemic to West Africa (found in OGD, Fig. 6b). Also, significant associations were found between the 3pA and 3pB inversions of *A. aegypti* and the 2Rj inversion of *An. gambiae* (Fig. 6b). Although we did not find correlations between the common inversions 1pA and 3qG, which are distributed throughout the African continent in *A. aegypti*, and inversions in *An. gambiae* in Africa, we found a strong association between the common African 2La inversion in *An. gambiae* and the 2pA inversion in *A. aegypti* in Brazil. Overall, these results indicate that some inversions nonrandomly capture similar sets of genes important for mosquito adaptation, suggesting a parallel evolution of the two species. Alternatively, these genomic regions may share properties that make them unstable leading to a higher-than-average rate of production of chromosomal rearrangements. Chromosomal inversions can be involved in parallel evolution in various organisms (Westram et al. 2022). Such parallel evolution is most likely to be detected in regions subjected to strong selection such as inversions.

Interestingly, in two populations of *A. aegypti* in Senegal, we found an unusual rearrangement, a triple inversion on arm 1q comprising three overlapping inversions 1qD, 1qF, and 1qE. Similarly, the inversion 3L1 is represented by a combination of at least two overlapping inversions in the malaria mosquito *Anopheles messeae* (Artemov et al. 2021). This double inversion is widespread in natural

populations in Eurasia but the two single inversions inside 3L1 were never found separately in nature (Brusentsov et al. 2023). Such overlapping chromosomal inversions should lead to a greater reduction of recombination compared to single inversions. Indeed, the triple inversion 1qE overlaps with the highest peaks of genetic divergence between strains from West Africa (Rose et al. 2020). Such suppression of recombination may cause differentiation of the gene arrangements and may accelerate the accumulation of fixed genetic differences among populations. Thus, our discovery of chromosomal inversions in *A. aegypti* will assist in adequate interpretation of population genomic data in this species.

According to recent investigations, *A. aegypti* likely originated in the islands of the Southwest Indian Ocean after diverging from its closest relative *A. mascarensis* around 7 MYA and invading Africa around 85,000 years ago (Soghigian et al. 2020). Beginning about 5,000 years ago, two forms began to emerge in West Africa, one remaining in its native forest ecotone habitat and the other beginning to use human settlements to survive long dry periods (Rose et al. 2023). This latter form was preadapted to life aboard ships and began to spread around the tropical and subtropical regions in the world about 500 years ago during slave trade period. Gradually, this human-associated form acquired the morphological and behavioral traits that we now associate with subspecies *Aaa* (Mattingly 1957; Brown et al. 2011; Brown et al. 2014; McBride et al. 2014; Gloria-Soria et al. 2016; Powell et al. 2018; Rose et al. 2020). Our study revealed a striking difference between African inversion-rich, obviously *Aaf* populations and non-African inversion-poor *Aaa* populations supporting a derived status of non-African populations versus African populations of *A. aegypti*. Although the total number of strains examined was almost the same for African and non-African populations (12 vs. 11, respectively), most inversions were found in African strains (15 vs. 3). Interestingly, there was no overlap between inversions found in African and non-African populations. This could be due to insufficient sampling in our study or, perhaps, new inversions arose or drifted to high frequency during population bottlenecks in *Aaa* over the relatively short period (≈500 years) since it escaped Africa. Thus, the inversion data add to the growing support for the genetic distinctness of *Aaa* and *Aaf*, implying a single out of Africa event (Brown et al. 2014; Gloria-Soria et al. 2016; Kotsakiozi et al. 2018; Powell et al. 2018).

Could inversions provide insights on the geographic origin of the introduction of *A. aegypti* outside of Africa? The ancestral proto-*Aaa* form should have a similar chromosomal arrangement to non-African populations with a low number of inversions or no inversions in their genome. While there are many endemic inversions segregating in West Africa, they have low frequency in some strains in northern Senegal where proto-*Aaa* has been found. For example, many mosquitoes from the human-preferring NGO population have no inversions. Our data are, thus, consistent with the idea that proto-*Aaa* arose in West Africa and was then perhaps introduced to other coastal African slave trading ports, such as in Angola, where they mixed further with local populations before migrating to the Americas. Coastal Angola as a place of proximate origin of the non-African *Aaa* has been proposed partly due to the large amount of slave-trade from the place that is coastal Angola today (Kotsakiozi et al. 2018; Rose et al. 2023).

In addition, we tested whether geographical clusters associated with the two most common inversions in Africa, 1pA and 3qG, followed the patterns of population structure in *A. aegypti* or whether these clusters have their own geographical patterns, suggesting involvement of these inversions in climatic or ecological adaptations of the mosquitoes. Frequencies of the two common inversions were estimated in 24 populations across Africa using the SNP-based genotyping approach developed in this study and reviled presence of four major clusters. Although we did not find a direct correlation between the levels of Aaa admixture and inversions, overall these data overlap with the observation of the presence of three major geographical clusters in Africa associated with West, East, and Central Africa (Rose et al. 2020). The presence of an additional coastal cluster in West Africa may suggest a role for these inversions in climate adaptation. However, better sampling is needed to determine the impact of inversions on the neutrality assumptions made for *A. aegypti* population genetics.

To evaluate how inversions may potentially affect traits important in disease transmission, we attempted to correlate locations of the chromosomal inversions with the positions of clusters of chemoreceptor genes involved in smell and taste (Matthews et al. 2018) and QTL related to levels of pathogen infections (Bosio et al. 2000; Severson et al. 2002; Timoshevskiy et al. 2013). We found significant overlap of the 1qF inversion, which is endemic in West Africa, with clusters of OR genes located close to the telomere on 1q (Matthews et al. 2018). As was shown before, this region overlaps with the highest peaks of SNP differences between strains in West Africa (Rose et al. 2020), which includes a gene Or4 that was previously linked to preference for human odors (McBride et al. 2014). Interestingly, inversion 2pA, which colocalized with the location of QTL implicated to affect multiple pathogen infections including dengue, filariasis, and avian malaria (Timoshevskiy et al. 2013), is a homologous to inversion 2La in *An. gambiae*, which is known to be associated with malaria transmission (Riehle et al. 2017). These results suggest that chromosomal inversions can potentially regulate the behavior of mosquitoes related to their ability to recognize humans as potential hosts and to transmit epidemiologically important pathogens.

Methods

Mosquito colonies

Information about mosquito colonies and collections is summarized in supplementary table S1, Supplementary Material online (Severson et al. 2002; Garcia-Luna et al. 2018; Matthews et al. 2018; Rose et al. 2020; Metz et al. 2023). The Hi-C analyses included 23 strains of *A. aegypti*, which were recently colonized (supplementary table S1, Supplementary Material online). Of these, 12 strains were from 6 African countries across the species' native range (Senegal, Burkina Faso, Nigeria, Gabon, Uganda, and Kenya), while 11 strains were from 5 non-African countries (Mexico, United States, Brazil, Thailand, and Malaysia). The SNP-genotyping approach included 32 strains that were previously sequenced using WGS (supplementary table S4, Supplementary Material online, Rose et al. 2020). In addition, two laboratory strains of *A. aegypti* (Liverpool and inbred Liverpool strain, RU3) and *A. mascarensis*, a closely related species of *A. aegypti,* from Mauritius Island, were also utilized. Colonies were kept under standard conditions in incubators (Benedict and Dotson 2015).

Hi-C inversion detection

To discover chromosomal inversions, 2,235 adults from 20 strains and >6,000 embryos from 6 strains were used to build 49 Hi-C libraries (supplementary table S1, Supplementary Material online). Two Hi-C libraries were made for most strains, except for three strains (MONT, GUER, and RU3), for which only one library each was constructed. We first utilized the in situ Hi-C protocol for library preparation that was developed for mosquito embryos and described previously (Lukyanchikova et al. 2022a). Each replicate was made from more than 1,000 embryos. We then applied the Arima-Hi-C + High Coverage kit (Arima Genomics, Carlsbad, CA, USA) for the adult stage of mosquitoes. Most of the adults used here were males, which was needed for the equal capturing of both sex-determining chromosome 1, with exception for two Mexican strains (GUER and MONT) where both sexes were included due to the low amount of field collected materials. Adult mosquitoes were 1- to 3-day old. Hi-C libraries were prepared according to the protocols provided by the company (Arima Genomics, Carlsbad, CA, USA). The libraries were sequenced on the Illumina platform to get an approximate 50× coverage for each strain. For Hi-C heatmap development, sequence quality assessment was performed using FastQC software v.0.12.1 (Andrews 2010). The reads were aligned to the AaegL5 genome (Matthews et al. 2018) and Juicer Pipeline (Durand et al. 2016) was used to build the contact matrices and Hi-C heatmaps. A Juicebox software (Durand et al. 2016) was employed to visualize and compare heatmaps. Inversion identification was performed based on visual inspection of Hi-C maps as was done previously (Lukyanchikova et al. 2022b). Chromatin contact maps were built for each *A. aegypti* strain and inspected for long-range interactions. Long-distance contacts with a butterfly-like pattern were considered indicative of inversions.

Probe preparation and FISH

The probes for FISH were designed based on gene exons or cDNA fragments of longer than 3.5 kb inside of the inversions according to breakpoints predicted by the Hi-C maps. These fragments were synthesized by PCR (supplementary table S2, Supplementary Material online) and cloned in pBluescript SK (+) plasmid. Successful clones were validated by Sanger sequencing at the SB RAS Genomics Core Facility.

Chromosomal preparations were followed as described elsewhere (Sharakhova et al. 2011a; Liang et al. 2022). Imaginal discs were dissected from 4th instar larvae. Good chromosome preparations were selected for FISH under an Olympus CX41 microscope (Olympus America, Inc., Melville, NY, USA) and FISH was performed using standard protocols (Timoshevskiy et al. 2012; Sharakhova et al. 2019). Purified plasmids were labeled with Cy3- or Cy5-dUTP (Enzo Life Sciences Inc., Farmingdale, NY, USA) using a nick translation method. After FISH, slides were analyzed and documented using a Zeiss AXIO fluorescent microscope with an Axiocam 506 mono digital camera (Carl Zeiss AG, Oberkochen, Germany) and a Zeiss LSM 880 Confocal Microscope (Carl Zeiss Microimaging, Inc., Thornwood, NY, USA). Previously described methods were utilized for probe mapping (Sharakhova et al. 2019). The FISH data are summarized in supplementary table S3, Supplementary Material online.

Identification of SNPs specific for 1pA and 3qG inversions

To identify putative inversion-diagnostic SNPs for the two most widespread inversions, 1pA and 3qG, principal components analysis (PCA) of 393 previously published *A. aegypti* genomes from Africa (Rose et al. 2020) was utilized. A two-step process was applied to minimize the effects of population structure. First, a PCA was conducted on the target genomic regions in a sample of individuals from Southern Senegal (BTT, KED, MIN, and PKT populations), where Hi-C analyses indicated the inversions should be polymorphic. A scatter plot of the first two principal components was visually inspected to confirm a bimodal or trimodal distribution of points along the first principal component, corresponding to different inversion genotypes. A trimodal distribution included standard (wildtype) homozygotes, inversion heterozygotes, and inverted homozygotes and was expected for common inversions.

A bimodal distribution represented standard homozygotes and inversion heterozygotes only and was expected for rare inversions which were not present in the homozygous state. Second, we examined loadings on the first principal component, and selected the set of SNPs with loadings close to the highest observed absolute value for further analysis across the full set of 393 individuals (79 SNPs for 1pA, 67 for 3qG), and the inversion genotype was estimated by taking the consensus genotype across these putatively inversion-linked SNPs. We then tested all SNPs across the putative inversion region for their correlation with the estimated karyotype. Putative diagnostic SNPs were selected based on: (i) perfect for inversion 3qG or near-perfect for inversion 1pA correlation with the putative karyotype (Pearson correlation >0.99); and (ii) distributions among populations corresponding to those identified from prior Hi-C analyses (Table 2).

Cluster analysis of the 1pA and 3qG inversion frequencies

Hierarchical clustering analysis was performed using the frequencies of chromosomal inversions 1pA and 3qG at the population level to infer and visualize the relationship between the species and populations using Package for R "stats" (R_Core_Team 2021). Frequencies of the chromosomal inversions were determined based on SNP-genotyping approach as described above based on previously published whole-genome sequences (WGS) of individual mosquitoes from seven countries in Africa and two countries outside of Africa (Rose et al. 2020). WGS from populations KAR and MASC were excluded from analysis because of the small number of individuals (two and four). The final analysis included 26 locations because in four different cases nearby (<50 km) populations with low numbers of mosquitoes were merged (supplementary table S4, Supplementary Material online). This populations marked by apostrophe in population ID. The reliability of data clustering was assessed using the "pvclust" package for R (Suzuki and Shimodaira 2006). The data were resampled 100 times and the similarity of different clustering variants was assessed using methods published elsewhere (Shimodaira 2002; Shimodaira 2004). The average values of these similarities were used as an indicator of cluster stability.

Colocalization of inversions with chemoreceptor genes and quantitative trait loci related to vector competence

Colocalization of inversions with chemoreceptor genes (Matthews et al. 2018) and QTL, associated with mosquito competence for key pathogens (Bosio et al. 2000; Severson et al. 2002; Timoshevskiy et al. 2013) was determined. First, the numbers of each type genes inside of the inversion were identified (denoted as k). Then, the statistical significance of increased density of OR, GR, and IR genes and QTL inside of the inversions was tested against the uniform distribution of them along the chromosomes. P-values were calculated as the upper tails of binomial distributions, i.e. $P(X \geq k) = 1-\mathrm{CDF}(k-1, B(n, p)) = 1- I_{1-p}(n-k+1, k)$, where $p = l/L$, $CDF(k-1, B(n, p))$ is the cumulative distribution function of binomial distribution B with parameters p and n, I is the incomplete beta function, l is the inversion length, L is the chromosome length, and n is the number of genes on the chromosome, $(n, k, l, L) \in \mathbb{Z}$. The correction for multiple comparisons P-values was calculated using the Benjamini–Hochberg method in the "stats" R package (Benjamini and Hochberg 1995) (supplementary table S5, Supplementary Material online). We applied the same approach to determine overlap between inversions and QTL associated with vector competence to different infections (supplementary table S5, Supplementary Material online).

In addition, the chemoreceptor genes were combined into evolutionary clusters to exclude the negative effect of the cluster organization of chemoreceptor genes in the mosquito genomes on the significance of the results. For this purpose, phylogenetic trees (supplementary figs. S7 to S9, Supplementary Material online) were constructed for chemoreceptor genes of *A. aegypti*, as described previously (Ryazansky et al. 2024). Branches with closely related genes on these trees were identified and combined into clusters of evolutionary related and closely located genes (supplementary figs. S7 to S9, Supplementary Material online, supplementary table S6, Supplementary Material online). Each such cluster of chemoreceptor genes interpreted as one gene. The threshold value was decreased until the distribution of genes and clusters was uniform. The compliance with an uniform distribution tested using the DistributionFitTest function from the Mathematica v. 13.3 program (Wolfram Research 2023). P-values were calculated as described previously considering each cluster of chemoreceptor genes as one gene (supplementary table S7, Supplementary Material online).

Finally, a permutation test was used to calculate nonrandom distribution of inversions in respect to chemoreceptor genes (Cabrera et al. 2012). A total of 100 circular chromosome permutations, in which a single random offset was drawn from a uniform distribution across the length of each chromosome, was added to all chemoreceptor positions within a given permutation. Then the modulo of the resulting position with the length of the chromosome was used to assign the new position of each chemoreceptor gene by "rotating" the position of all chemoreceptor genes together, preserving the relative distribution of chemoreceptor genes within the chromosome in each permutation. The number of chemoreceptor gene-inversion intersections in each permutation using *bedtools intersect* was then calculated.

Overlapping inversions in the *A. aegypti* and *An. gambiae* genomes

To determine if chromosomal inversions in *A. aegypti* and in *An. gambiae* captured similar sets of genes, we first identified single copy orthologs between the species using OrthoFinder software (Emms and Kelly 2019) with default settings. The genomic positions of the inversions were identified based on previously published data (Sharakhov et al. 2006; Coulibaly et al. 2007; George et al. 2010; Lobo et al. 2010) summarized in supplementary table S8, Supplementary Material online. The identified single-copy orthologs were overlapped with the genomic coordinates between two species using the BEDTools function *intersect-loj* (Quinlan 2014). To calculate the significance of pairwise inversion overlaps between species, we used a hypergeometric test based on the single-copy orthologs inside and outside of each inversion. The raw *P*-values were adjusted with the Benjamini–Hochberg method. Calculations were performed using the R package "GeneOverlap" (shenlab-sinai 2023). Circos software was used to visualize the common regions with inversion polymorphism among the species (Krzywinski et al. 2009).

Supplementary Material

Supplementary material is available at *Genome Biology and Evolution* online.

Acknowledgments

We thank Janet Webster from Virginia Polytechnic and State University, VA, USA for editing manuscript text and Teoh Guat Ney from the Institute for Medical Research, National Institutes of Health, Ministry of Health, Kuala Lumpur, Malaysia for supporting mosquito collections in Malaysia.

Author Contributions

Conceptualization: M.V.S., C.S.M., I.V.S., and J.R.P.; methodology: J.L., N.R., I.V.S., and V.L.; investigation: J.L., N.R., I.I.B., D.A.K., A.A.Y., Y.F., A.S.; writing—original draft preparation: M.V.S., J.L., N.R., I.V.S., I.I.B., D.A.K., A.A.Y., J.R.P., C.S.M.; writing—review and editing: M.V.S., J.L., N.R., K.D.A.; supervision, M.V.S., C.S.M.; project administration: M.V.S., E.M.B.; funding acquisition: M.V.S., I.V.S., E.M.B., mosquito collections: Z.T., M.S., J.L., A.B., O.A., D.A., C.G.A., B.W.A., N.W.A., A.G-S, W.C.B. All authors have read and agreed to the published version of the manuscript.

Funding

The project was supported by multiple funding sources. The most significant support was received from NIH/NIAID National Institutes of Health/National Institute of Allergy and Infectious Diseases funding R21 AI146528 and R21 AI174052 to M.V.S. and also from the USDA National Institute of Food and Agriculture U.S. Department of Agriculture, Hatch project VA-160058 to M.V.S. Bioinformatic analyses of the Hi-C libraries and probe development for the inversion validation was supported by the FWNR-2022-0015 project of the Institute of Cytology and Genetics, Federal Research Center Institute of Cytology and Genetics, Siberian Branch of Russian Academy of Sciences, Novosibirsk, Russia.

Conflict of Interest

The authors declare that they have no competing interests.

Data Availability

All raw and processed sequencing data generated in this study have been submitted to the NCBI Gene Expression Omnibus (GEO; https://www.ncbi.nlm.nih.gov/geo/) under accession number GSE243024. The Hi-C Illumina data generated in this study have been submitted to the NCBI BioProject database (https://www.ncbi.nlm.nih.gov/bioproject/) under accession number PRJNA1003935.

Literature Cited

Andrews S. FastQC: a quality control tool for high throughput sequence data. Babraham Institute; 2010.

Arensburger P, Megy K, Waterhouse RM, Abrudan J, Amedeo P, Antelo B, Bartholomay L, Bidwell S, Caler E, Camara F, et al. Sequencing of *Culex quinquefasciatus* establishes a platform for mosquito comparative genomics. Science. 2010:330(6000):86–88. https://doi.org/10.1126/science.1191864.

Artemov GN, Fedorova VS, Karagodin DA, Brusentsov II, Baricheva EM, Sharakhov IV, Gordeev MI, Sharakhova MV. New cytogenetic photomap and molecular diagnostics for the cryptic species of the malaria mosquitoes *Anopheles messeae* and *Anopheles daciae* from Eurasia. Insects. 2021:12(9):835. https://doi.org/10.3390/insects12090835.

Aubry F, Dabo S, Manet C, Filipovic I, Rose NH, Miot EF, Martynow D, Baidaliuk A, Merkling SH, Dickson LB, et al. Enhanced Zika virus susceptibility of globally invasive *Aedes aegypti* populations. Science. 2020:370(6519):991–996. https://doi.org/10.1126/science.abd3663.

Ayala D, Acevedo P, Pombi M, Dia I, Boccolini D, Costantini C, Simard F, Fontenille D. Chromosome inversions and ecological plasticity in the main African malaria mosquitoes. Evolution. 2017:71(3):686–701. https://doi.org/10.1111/evo.13176.

Ayala D, Ullastres A, Gonzalez J. Adaptation through chromosomal inversions in *Anopheles*. Front Genet. 2014:5:129. https://doi.org/10.3389/fgene.2014.00129.

Ayala FJ, Coluzzi M. Chromosome speciation: humans, Drosophila, and mosquitoes. Proc Natl Acad Sci U S A. 2005:102(suppl_1):6535–6542. https://doi.org/10.1073/pnas.0501847102.

Benedict M, Dotson EM. 2015. Methods in Anopheles research. https://www.beiresources.org/Portals/2/VectorResources/2016%20Methods%20in%20Anopheles%20Research%20full%20manual.pdf.

Benjamini Y, Hochberg Y. Controlling the false discovery rate: a practical and powerful approach to multiple testing. J R Stat Soc Series B Stat Methodol. 1995:57:129–300. https://doi.org/10.1111/j.2517-6161.1995.tb02031.x.

Berdan EL, Barton NH, Butlin R, Charlesworth B, Faria R, Fragata I, Gilbert KJ, Jay P, Kapun M, Lotterhos KE, et al. How chromosomal inversions reorient the evolutionary process. J Evol Biol. 2023:36:1761–1782. https://doi.org/10.1111/jeb.14242.

Berdan EL, Flatt T, Kozak GM, Lotterhos KE, Wielstra B. Genomic architecture of supergenes: connecting form and function. Philos Trans R Soc Lond B Biol Sci. 2022:377(1856):20210192. https://doi.org/10.1098/rstb.2021.0192.

Bernhardt SA, Blair C, Sylla M, Bosio C, Black WC. Evidence of multiple chromosomal inversions in *Aedes aegypti formosus* from Senegal. Insect Mol Biol. 2009:18(5):557–569. https://doi.org/10.1111/j.1365-2583.2009.00895.x.

Bosio CF, Fulton RE, Salasek ML, Beaty BJ, Black WC. Quantitative trait loci that control vector competence for dengue-2 virus in the mosquito *Aedes aegypti*. Genetics. 2000:156(2):687–698. https://doi.org/10.1093/genetics/156.2.687.

Brown JE, Evans BR, Zheng W, Obas V, Barrera-Martinez L, Egizi A, Zhao H, Caccone A, Powell JR. Human impacts have shaped historical and recent evolution in *Aedes aegypti*, the dengue and yellow fever mosquito. Evolution. 2014:68(2):514–525. https://doi.org/10.1111/evo.12281.

Brown JE, McBride CS, Johnson P, Ritchie S, Paupy C, Bossin H, Lutomiah J, Fernandez-Salas I, Ponlawat A, Cornel AJ, et al. Worldwide patterns of genetic differentiation imply multiple 'domestications' of *Aedes aegypti*, a major vector of human diseases. Proc Biol Sci. 2011:278(1717):2446–2454. https://doi.org/10.1098/rspb.2010.2469.

Brusentsov II, Gordeev MI, Yurchenko AA, Karagodin DA, Moskaev AV, Hodge JM, Burlak VA, Artemov GN, Sibataev AK, Becker N, et al. Patterns of genetic differentiation imply distinct phylogeographic history of the mosquito species *Anopheles messeae* and *Anopheles daciae* in Eurasia. Mol Ecol. 2023:32(20):5609–5625. https://doi.org/10.1111/mec.17127.

Cabrera CP, Navarro P, Huffman JE, Wright AF, Hayward C, Campbell H, Wilson JF, Rudan I, Hastie ND, Vitart V, et al. Uncovering networks from genome-wide association studies via circular genomic permutation. G3 (Bethesda). 2012:2(9):1067–1075. https://doi.org/10.1534/g3.112.002618.

Campos J, Andrade CF, Recco-Pimentel SM. A technique for preparing polytene chromosomes from *Aedes aegypti* (Diptera, Culicinae). Mem Inst Oswaldo Cruz. 2003:98(3):387–390. https://doi.org/10.1590/S0074-02762003000300017.

Chakraborty A, Ay F. Identification of copy number variations and translocations in cancer cells from Hi-C data. Bioinformatics. 2018:34(2):338–345. https://doi.org/10.1093/bioinformatics/btx664.

Coluzzi M, Sabatini A, della Torre A, Di Deco MA, Petrarca V. A polytene chromosome analysis of the *Anopheles gambiae* species complex. Science. 2002:298(5597):1415–1418. https://doi.org/10.1126/science.1077769.

Corbett-Detig RB, Said I, Calzetta M, Genetti M, McBroome J, Maurer NW, Petrarca V, Della Torre A, Besansky NJ. Fine-mapping complex inversion breakpoints and investigating somatic pairing in the *Anopheles gambiae* species complex using proximity-ligation sequencing. Genetics. 2019:213(4):1495–1511. https://doi.org/10.1534/genetics.119.302385.

Coulibaly MB, Lobo NF, Fitzpatrick MC, Kern M, Grushko O, Thaner DV, Traore SF, Collins FH, Besansky NJ. Segmental duplication implicated in the genesis of inversion 2Rj of *Anopheles gambiae*. PLoS One. 2007:2(9):e849. https://doi.org/10.1371/journal.pone.0000849.

Crawford JE, Balcazar D, Redmond S, Rose NH, Youd HA, Lucas ER, Ali RSM, Alnazawi A, Badolo A, Chen C-H, et al. Sequencing 1206 genomes reveals origin and movement of Aedes aegypti driving increased dengue risk. bioRxiv 604830. https://doi.org/10.1101/2024.07.23.604830, 24 July 2024, preprint: not peer reviewed.

Dekker J, Rippe K, Dekker M, Kleckner N. Capturing chromosome conformation. Science. 2002:295(5558):1306–1311. https://doi.org/10.1126/science.1067799.

Dickson LB, Sanchez-Vargas I, Sylla M, Fleming K, Black WC. Vector competence in West African *Aedes aegypti* is flavivirus species and genotype dependent. PLoS Negl Trop Dis. 2014:8(10):e3153. https://doi.org/10.1371/journal.pntd.0003153.

Dickson LB, Sharakhova MV, Timoshevskiy VA, Fleming KL, Caspary A, Sylla M, Black WC. Reproductive incompatibility involving Senegalese *Aedes aegypti* (L) is associated with chromosome rearrangements. PLoS Negl Trop Dis. 2016:10(4):e0004626. https://doi.org/10.1371/journal.pntd.0004626.

Durand NC, Robinson JT, Shamim MS, Machol I, Mesirov JP, Lander ES, Aiden EL. Juicebox provides a visualization system for Hi-C contact maps with unlimited zoom. Cell Syst. 2016:3(1):99–101. https://doi.org/10.1016/j.cels.2015.07.012.

Emms DM, Kelly S. OrthoFinder: phylogenetic orthology inference for comparative genomics. Genome Biol. 2019:20(1):238. https://doi.org/10.1186/s13059-019-1832-y.

Engreitz JM, Agarwala V, Mirny LA. Three-dimensional genome architecture influences partner selection for chromosomal translocations in human disease. PLoS One. 2012:7(9):e44196. https://doi.org/10.1371/journal.pone.0044196.

Faria NR, Azevedo Rdo S, Kraemer MU, Souza R, Cunha MS, Hill SC, Theze J, Bonsall MB, Bowden TA, Rissanen I, et al. Zika virus in the Americas: early epidemiological and genetic findings. Science. 2016:352(6283):345–349. https://doi.org/10.1126/science.aaf5036.

Ferguson-Smith MA, Trifonov V. Mammalian karyotype evolution. Nat Rev Genet. 2007:8(12):950–962. https://doi.org/10.1038/nrg2199.

Fijman NS, Yee DA. Mapping yellow fever epidemics as a potential indicator of the historical range of *Aedes aegypti* in the United States. Mem Inst Oswaldo Cruz. 2022:117:e220306. https://doi.org/10.1590/0074-02760220306.

Fontenille D, Powell JR. From anonymous to public enemy: how does a mosquito become a feared arbovirus vector? Pathogens. 2020:9(4):1–11. https://doi.org/10.3390/pathogens9040265.

Fuller ZL, Koury SA, Phadnis N, Schaeffer SW. How chromosomal rearrangements shape adaptation and speciation: case studies in *Drosophila pseudoobscura* and its sibling species *Drosophila persimilis*. Mol Ecol. 2019:28(6):1283–1301. https://doi.org/10.1111/mec.14923.

Garcia-Luna SM, Weger-Lucarelli J, Ruckert C, Murrieta RA, Young MC, Byas AD, Fauver JR, Perera R, Flores-Suarez AE, Ponce-Garcia G, et al. Variation in competence for ZIKV transmission by *Aedes aegypti* and *Aedes albopictus* in Mexico. PLoS Negl Trop Dis. 2018:12(7):e0006599. https://doi.org/10.1371/journal.pntd.0006599.

George P, Sharakhova MV, Sharakhov IV. High-resolution cytogenetic map for the African malaria vector *Anopheles gambiae*. Insect Mol Biol. 2010:19(5):675–682. https://doi.org/10.1111/j.1365-2583.2010.01025.x.

Gloria-Soria A, Ayala D, Bheecarry A, Calderon-Arguedas O, Chadee DD, Chiappero M, Coetzee M, Elahee KB, Fernandez-Salas I, Kamal HA, et al. Global genetic diversity of *Aedes aegypti*. Mol Ecol. 2016:25(21):5377–5395. https://doi.org/10.1111/mec.13866.

Gray EM, Rocca KA, Costantini C, Besansky NJ. Inversion 2La is associated with enhanced desiccation resistance in *Anopheles gambiae*. Malar J. 2009:8(1):215. https://doi.org/10.1186/1475-2875-8-215.

Gubler DJ. The 20th century re-emergence of epidemic infectious diseases: lessons learned and future prospects. Med J Aust. 2012:196(5):293–294. https://doi.org/10.5694/mja12.10104.

Harewood L, Kishore K, Eldridge MD, Wingett S, Pearson D, Schoenfelder S, Collins VP, Fraser P. Hi-C as a tool for precise detection and characterisation of chromosomal rearrangements and copy number variation in human tumours. Genome Biol. 2017:18(1):125. https://doi.org/10.1186/s13059-017-1253-8.

Holt RA, Subramanian GM, Halpern A, Sutton GG, Charlab R, Nusskern DR, Wincker P, Clark AG, Ribeiro JM, Wides R, et al. The genome sequence of the malaria mosquito *Anopheles gambiae*. Science. 2002:298(5591):129–149. https://doi.org/10.1126/science.1076181.

Huang K, Rieseberg LH. Frequency, origins, and evolutionary role of chromosomal inversions in plants. Front Plant Sci. 2020:11:296. https://doi.org/10.3389/fpls.2020.00296.

Jay P, Joron M. The double game of chromosomal inversions in a neotropical butterfly. C R Biol. 2022:345(1):57–73. https://doi.org/10.5802/crbiol.73.

Kitzmiller JB. Genetics, cytogenetics, and evolution of mosquitoes. In: Caspari EW, editor. Advances in genetics, Vol. 18. Elsevier Inc; 1976. p. 315–433.

Kosuthova K, Solc R. Inversions on human chromosomes. Am J Med Genet A. 2023:191(3):672–683. https://doi.org/10.1002/ajmg.a.63063.

Kotsakiozi P, Evans BR, Gloria-Soria A, Kamgang B, Mayanja M, Lutwama J, Le Goff G, Ayala D, Paupy C, Badolo A, et al. Population structure of a vector of human diseases: *Aedes aegypti* in its ancestral range, Africa. Ecol Evol. 2018:8(16):7835–7848. https://doi.org/10.1002/ece3.4278.

Krimbas CB, Powell JR. Drosophila inversion polymorphism. CRC Press; 1992.

Krzywinski M, Schein J, Birol I, Connors J, Gascoyne R, Horsman D, Jones SJ, Marra MA. Circos: an information aesthetic for comparative genomics. Genome Res. 2009:19(9):1639–1645. https://doi.org/10.1101/gr.092759.109.

Lanzaro GC, Toure YT, Carnahan J, Zheng L, Dolo G, Traore S, Petrarca V, Vernick KD, Taylor CE. Complexities in the genetic structure of *Anopheles gambiae* populations in West Africa as revealed by microsatellite DNA analysis. Proc Natl Acad Sci U S A. 1998:95(24):14260–14265. https://doi.org/10.1073/pnas.95.24.14260.

Liang J, Bondarenko SM, Sharakhov IV, Sharakhova MV. Obtaining polytene, meiotic, and mitotic chromosomes from mosquitoes for cytogenetic analysis. Cold Spring Harb Protoc. 2022:2022:591–598. https://doi.org/10.1101/pdb.prot107872.

Lieberman-Aiden E, van Berkum NL, Williams L, Imakaev M, Ragoczy T, Telling A, Amit I, Lajoie BR, Sabo PJ, Dorschner MO, et al. Comprehensive mapping of long-range interactions reveals folding principles of the human genome. Science. 2009:326(5950):289–293. https://doi.org/10.1126/science.1181369.

Lobo NF, Sangare DM, Regier AA, Reidenbach KR, Bretz DA, Sharakhova MV, Emrich SJ, Traore SF, Costantini C, Besansky NJ, et al. Breakpoint structure of the *Anopheles gambiae* 2Rb chromosomal inversion. Malar J. 2010:9(1):293. https://doi.org/10.1186/1475-2875-9-293.

Lorenz L, Beaty BJ, Aitken TH, Wallis GP, Tabachnick WJ. The effect of colonization upon *Aedes aegypti* susceptibility to oral infection with yellow fever virus. Am J Trop Med Hyg. 1984:33(4):690–694. https://doi.org/10.4269/ajtmh.1984.33.690.

Love RR, Pombi M, Guelbeogo MW, Campbell NR, Stephens MT, Dabire RK, Costantini C, Della Torre A, Besansky NJ. Inversion genotyping in the *Anopheles gambiae* complex using high-throughput array and sequencing platforms. G3 (Bethesda). 2020:10(9):3299–3307. https://doi.org/10.1534/g3.120.401418.

Love RR, Redmond SN, Pombi M, Caputo B, Petrarca V, Della Torre A, Anopheles gambiae 1000 Genomes Consortium, Besansky NJ. In silico karyotyping of chromosomally polymorphic malaria mosquitoes in the *Anopheles gambiae* complex. G3 (Bethesda). 2019:9(10):3249–3262. https://doi.org/10.1534/g3.119.400445.

Love RR, Steele AM, Coulibaly MB, Traore SF, Emrich SJ, Fontaine MC, Besansky NJ. Chromosomal inversions and ecotypic differentiation in *Anopheles gambiae:* the perspective from whole-genome sequencing. Mol Ecol. 2016:25(23):5889–5906. https://doi.org/10.1111/mec.13888.

Lukyanchikova V, Fishman V, Sharakhov I. 2022a. In situ Hi-C for mosquito embryos. https://www.protocols.io/.

Lukyanchikova V, Nuriddinov M, Belokopytova P, Taskina A, Liang J, Reijnders M, Ruzzante L, Feron R, Waterhouse RM, Wu Y, et al. *Anopheles* mosquitoes reveal new principles of 3D genome organization in insects. Nat Commun. 2022b:13(1):1960. https://doi.org/10.1038/s41467-022-29599-5.

Matthews BJ, Dudchenko O, Kingan SB, Koren S, Antoshechkin I, Crawford JE, Glassford WJ, Herre M, Redmond SN, Rose NH, et al. Improved reference genome of *Aedes aegypti* informs arbovirus vector control. Nature. 2018:563(7732):501–507. https://doi.org/10.1038/s41586-018-0692-z.

Mattingly PF. Genetical aspects of the *Aedes aegypti* problem. I. Taxonomy and bionomics. Ann Trop Med Parasitol. 1957:51(4):392–408. https://doi.org/10.1080/00034983.1957.11685829.

McBride CS. Genes and odors underlying the recent evolution of mosquito preference for humans. Curr Biol. 2016:26(1):R41–R46. https://doi.org/10.1016/j.cub.2015.11.032.

McBride CS, Baier F, Omondi AB, Spitzer SA, Lutomiah J, Sang R, Ignell R, Vosshall LB. Evolution of mosquito preference for humans linked to an odorant receptor. Nature. 2014:515(7526):222–227. https://doi.org/10.1038/nature13964.

Metz HC, Miller AK, You J, Akorli J, Avila FW, Buckner EA, Kane P, Otoo S, Ponlawat A, Triana-Chavez O, et al. Evolution of a mosquito's hatching behavior to match its human-provided habitat. Am Nat. 2023:201(2):200–214. https://doi.org/10.1086/722481.

More DF. Hybridization and mating behavior in *Aedes aegypti* (Diptera, Culicidae). J Med Entomol. 1979:16(3):223–226. https://doi.org/10.1093/jmedent/16.3.223.

Nabel GJ, Zerhouni EA. Once and future epidemics: Zika virus emerging. Sci Transl Med. 2016:8(330):d332. https://doi.org/10.1126/scitranslmed.aaf4548.

Olagnier D, Amatore D, Castiello L, Ferrari M, Palermo E, Diamond MS, Palamara AT, Hiscott J. Dengue virus immunopathogenesis: lessons applicable to the emergence of Zika virus. J Mol Biol. 2016:428(17):3429–3448. https://doi.org/10.1016/j.jmb.2016.04.024.

Oliveira da Silva W, Malcher SM, Ferguson-Smith MA, O'Brien PCM, Rossi RV, Geise L, Pieczarka JC, Nagamachi CY. Chromosomal rearrangements played an important role in the speciation of rice rats of genus Cerradomys (Rodentia, Sigmodontinae, Oryzomyini). Sci Rep. 2024:14(1):545. https://doi.org/10.1038/s41598-023-50861-3.

Powell JR. Mosquitoes on the move. Science. 2016a:354(6315):971–972. https://doi.org/10.1126/science.aal1717.

Powell JR. New contender for most lethal animal. Nature. 2016b:540(7634):525. https://doi.org/10.1038/540525c.

Powell JR, Gloria-Soria A, Kotsakiozi P. Recent history of *Aedes aegypti*: vector genomics and epidemiology records. Bioscience. 2018:68(11):854–860. https://doi.org/10.1093/biosci/biy119.

Powell JR, Tabachnick WJ. History of domestication and spread of *Aedes aegypti*–a review. Mem Inst Oswaldo Cruz. 2013:108(suppl 1):11–17. https://doi.org/10.1590/0074-0276130395.

Quinlan AR. BEDTools: the Swiss-army tool for genome feature analysis. Curr Protoc Bioinformatics. 2014:47(1):11.12.1–11.12.34. https://doi.org/10.1002/0471250953.bi1112s47.

R_Core_Team. R: a language and environment for statistical computing. Vienna: R Foundation for Statistical Computing; 2021.

Redmond SN, Sharma A, Sharakhov I, Tu Z, Sharakhova M, Neafsey DE. Linked-read sequencing identifies abundant microinversions and

introgression in the arboviral vector *Aedes aegypti*. BMC Biol. 2020:18(1):26. https://doi.org/10.1186/s12915-020-0757-y.
Riehle MM, Bukhari T, Gneme A, Guelbeogo WM, Coulibaly B, Fofana A, Pain A, Bischoff E, Renaud F, Beavogui AH, et al. The *Anopheles gambiae* 2La chromosome inversion is associated with susceptibility to *Plasmodium falciparum* in Africa. Elife. 2017:6:e25813. https://doi.org/10.7554/eLife.25813.
Robinson JT, Turner D, Durand NC, Thorvaldsdottir H, Mesirov JP, Aiden EL. Juicebox.js provides a cloud-based visualization system for Hi-C data. Cell Syst. 2018:6(2):256–258.e1. https://doi.org/10.1016/j.cels.2018.01.001.
Rose NH, Badolo A, Sylla M, Akorli J, Otoo S, Gloria-Soria A, Powell JR, White BJ, Crawford JE, McBride CS. Dating the origin and spread of specialization on human hosts in *Aedes aegypti* mosquitoes. Elife. 2023:12:e83524. https://doi.org/10.7554/eLife.83524.
Rose NH, Sylla M, Badolo A, Lutomiah J, Ayala D, Aribodor OB, Ibe N, Akorli J, Otoo S, Mutebi JP, et al. Climate and urbanization drive mosquito preference for humans. Curr Biol. 2020:30(18):3570–3579.e6. https://doi.org/10.1016/j.cub.2020.06.092.
Ryazansky SS, Chen C, Potters M, Naumenko AN, Lukyanchikova V, Masri RA, Brusentsov II, Karagodin DA, Yurchenko AA, Dos Anjos VL, et al. The chromosome-scale genome assembly for the West Nile vector *Culex quinquefasciatus* uncovers patterns of genome evolution in mosquitoes. BMC Biol. 2024:22(1):16. https://doi.org/10.1186/s12915-024-01825-0.
Severson DW, Meece JK, Lovin DD, Saha G, Morlais I. Linkage map organization of expressed sequence tags and sequence tagged sites in the mosquito, *Aedes aegypti*. Insect Mol Biol. 2002:11(4):371–378. https://doi.org/10.1046/j.1365-2583.2002.00347.x.
Sharakhov IV, White BJ, Sharakhova MV, Kayondo J, Lobo NF, Santolamazza F, Della Torre A, Simard F, Collins FH, Besansky NJ. Breakpoint structure reveals the unique origin of an interspecific chromosomal inversion (2La) in the *Anopheles gambiae* complex. Proc Natl Acad Sci U S A. 2006:103(16):6258–6262. https://doi.org/10.1073/pnas.0509683103.
Sharakhova MV, Artemov GN, Timoshevskiy VA, Sharakhov IV. Physical genome mapping using fluorescence *in situ* hybridization with mosquito chromosomes. Methods Mol Biol. 2019:1858:177–194. https://doi.org/10.1007/978-1-4939-8775-7_13.
Sharakhova MV, Timoshevskiy VA, Yang F, Demin S, Severson DW, Sharakhov IV. Imaginal discs: a new source of chromosomes for genome mapping of the yellow fever mosquito *Aedes aegypti*. PLoS Negl Trop Dis. 2011a:5(10):e1335. https://doi.org/10.1371/journal.pntd.0001335.
Sharakhova MV, Xia A, Leman SC, Sharakhov IV. Arm-specific dynamics of chromosome evolution in malaria mosquitoes. BMC Evol Biol. 2011b:11(1):91. https://doi.org/10.1186/1471-2148-11-91.
shenlab-sinai. 2023. GeneOverlap: test and visualize gene overlaps. R package version 1.36.0. https://github.com/shenlab-sinai/GeneOverlap.
Shimodaira H. An approximately unbiased test of phylogenetic tree selection. Syst Biol. 2002:51(3):492–508. https://doi.org/10.1080/10635150290069913.
Shimodaira H. Approximately unbiased tests of regions using multistep-multiscale bootstrap resampling. Ann Stat. 2004:32(6):2616–2641. https://doi.org/10.1214/009053604000000823.
Simard F, Ayala D, Kamdem GC, Pombi M, Etouna J, Ose K, Fotsing JM, Fontenille D, Besansky NJ, Costantini C. Ecological niche partitioning between *Anopheles gambiae* molecular forms in Cameroon: the ecological side of speciation. BMC Ecol. 2009:9(1):17. https://doi.org/10.1186/1472-6785-9-17.
Soghigian J, Gloria-Soria A, Robert V, Le Goff G, Failloux AB, Powell JR. Genetic evidence for the origin of *Aedes aegypti*, the yellow fever mosquito, in the southwestern Indian Ocean. Mol Ecol. 2020:29(19):3593–3606. https://doi.org/10.1111/mec.15590.
Souza-Neto JA, Powell JR, Bonizzoni M. *Aedes aegypti* vector competence studies: a review. Infect Genet Evol. 2019:67:191–209. https://doi.org/10.1016/j.meegid.2018.11.009.
Stegniy VN. Population genetics and evolution of malaria mosquitoes. Tomsk State University Publisher; 1991.
Suzuki R, Shimodaira H. Pvclust: an R package for assessing the uncertainty in hierarchical clustering. Bioinformatics. 2006:22(12):1540–1542. https://doi.org/10.1093/bioinformatics/btl117.
Sylla M, Bosio C, Urdaneta-Marquez L, Ndiaye M, Black WC. Gene flow, subspecies composition, and dengue virus-2 susceptibility among *Aedes aegypti* collections in Senegal. PLoS Negl Trop Dis. 2009:3(4):e408. https://doi.org/10.1371/journal.pntd.0000408.
Tabachnick WJ. Nature, nurture and evolution of intra-species variation in mosquito arbovirus transmission competence. Int J Environ Res Public Health. 2013:10(1):249–277. https://doi.org/10.3390/ijerph10010249.
Tabachnick WJ, Wallis GP, Aitken TH, Miller BR, Amato GD, Lorenz L, Powell JR, Beaty BJ. Oral infection of *Aedes aegypti* with yellow fever virus: geographic variation and genetic considerations. Am J Trop Med Hyg. 1985:34(6):1219–1224. https://doi.org/10.4269/ajtmh.1985.34.1219.
Thompson MJ, Jiggins CD. Supergenes and their role in evolution. Heredity (Edinb). 2014:113(1):1–8. https://doi.org/10.1038/hdy.2014.20.
Timoshevskiy VA, Kinney NA, de Bruyn BS, Mao C, Tu Z, Severson DW, Sharakhov IV, Sharakhova MV. Genomic composition and evolution of *Aedes aegypti* chromosomes revealed by the analysis of physically mapped supercontigs. BMC Biol. 2014:12(1):27. https://doi.org/10.1186/1741-7007-12-27.
Timoshevskiy VA, Severson DW, Debruyn BS, Black WC, Sharakhov IV, Sharakhova MV. An integrated linkage, chromosome, and genome map for the yellow fever mosquito *Aedes aegypti*. PLoS Negl Trop Dis. 2013:7(2):e2052. https://doi.org/10.1371/journal.pntd.0002052.
Timoshevskiy VA, Sharma A, Sharakhov IV, Sharakhova MV. Fluorescent *in situ* hybridization on mitotic chromosomes of mosquitoes. J Vis Exp. 2012:67:e4215. https://doi.org/10.3791/4215.
van Berkum NL, Lieberman-Aiden E, Williams L, Imakaev M, Gnirke A, Mirny LA, Dekker J, Lander ES. Hi-C: a method to study the three-dimensional architecture of genomes. J Vis Exp. 2010:39:e1869. https://doi.org/10.3791/1869.
Wallis GP, Aitken TH, Beaty BJ, Lorenz L, Amato GD, Tabachnick WJ. Selection for susceptibility and refractoriness of *Aedes aegypti* to oral infection with yellow fever virus. Am J Trop Med Hyg. 1985:34(6):1225–1231. https://doi.org/10.4269/ajtmh.1985.34.1225.
Weaver SC, Costa F, Garcia-Blanco MA, Ko AI, Ribeiro GS, Saade G, Shi PY, Vasilakis N. Zika virus: history, emergence, biology, and prospects for control. Antiviral Res. 2016:130:69–80. https://doi.org/10.1016/j.antiviral.2016.03.010.
Westram AM, Faria R, Johannesson K, Butlin R, Barton N. Inversions and parallel evolution. Philos Trans R Soc Lond B Biol Sci. 2022:377(1856):20210203. https://doi.org/10.1098/rstb.2021.0203.
WHO. Dengue and severe dengue. Geneva, Switzerland: WHO; 2022.
Wolfram Research. Mathematica. Vol version 13.3. Champaign (Illinois): Wolfram Research; 2023.

Associate editor: Josefa Gonzalez